Solar Car Suspension Project

Sponsor:

Dr. Doig and PROVE Lab

Team Members:

Alex Power
aspower@calpoly.edu

Adam O'Camb
aocamb@calpoly.edu

Table of Contents

1. Introduction

Our primary goal as the solar car suspension team is to design the front and rear suspension systems for our solar powered vehicle. This is an interdisciplinary project provided by PROVE Lab. PROVE Lab is a Prototype Vehicle Laboratory started at Cal Poly that consists of over 70 people and 11 different majors. PROVE Lab's faculty advisor and our senior project sponsor is Graham Doig who has worked on two world record breaking solar cars. We are excited to be working alongside PROVE Lab and Dr. Doig on our senior project. The overall goal of the PROVE Lab solar car is to reach a speed of 65 miles per hour, which will break the world speed records for solar cars without batteries for both *Guinness Book of World Records* [1] and the FIA (International Federation of Automobiles) [2]. In order to break the record, the solar car must drive a flying start mile. The solar car will do two runs and the average speed over the two runs must be greater than the previous record in order to create a new world record. We will have as much distance as we want to get the vehicle up to speed before recording the mile. The car must also rely solely on solar power to reach maximum speed. Most solar cars that exist today are designed for cross-country races, but our goal is just to set the land speed record for a solar car. This means that our design will differ from the solar cars that exist today. We will be working alongside aerospace, structures, steering, and business teams to design the solar car. It will be essential that we stay in contact with each team to ensure compatibility in each part of the design.

2. Background

The suspension system for any car is designed to maximize the contact between the surface of the road and the car's tires, provide steering stability with improved handling, and maximize the comfort of the passengers [3]. These can be further explained in three main design concerns: road isolation, road holding, and cornering. Road isolation is the suspension system's ability to absorb energy from bumps and dissipate the energy to maximize the comfort of the passengers [3]. Road holding is defined as how well the car maintains contact with the road while accelerating and stopping. Vehicles tend to dip forward during braking and "squat" during acceleration which can reduce the tire's grip on the surface of the road [3]. The last design concern is the cornering ability of the vehicle. The suspension system must transfer the weight of the car from the high side to the low side effectively to ensure the car will not roll [3]. These design concerns can be accomplished by choosing the correct spring, damper, mounting points and style of car suspension.

The suspension system generally consists of three different parts: the spring/damper, the connection points, and the control arms. The spring and damper is chosen based on the customer requirements. A stiff spring and damper system is used in a car designed for a performance while a softer spring is used in cars designed for comfort [4]. Comfort and performance are inversely proportional and have to be optimized to meet the customer's overall requirements. In our car, performance will take overwhelming priority over driver comfort. One of the most important parts of the suspension system is the mounting points to the frame. Our mounting points must be designed concurrently with the structures team so that the design remains compatible. The control arms of the suspension connect the spring and damper and the mounting points. The control arm(s) also provide overall structural support and control the geometry and motion of the suspension. These must be designed precisely to provide a favorable suspension geometry as well as support the car and fit inside the frame above the wheels [5].

When designing a favorable suspension geometry, we have to consider effects of our geometry on bump steer, lateral scrub, and toe angle. Bump steer means that when the suspension moves vertically the wheels also turn. This occurs when the steering tie rod follows a different arc than the suspension control arms, causing the tie rod to push or pull the wheel when the suspension is compressed. To minimize bump steer, the hinges of the control arms and the tie rod must all be located along the same line (Line 2 in Figure 1). In addition, Imaginary lines drawn through the control arm(s) and tie rod must also intersect at the instant center. A visual explanation is shown in Figure 1. Lateral scrub is lateral movement of the wheel when the suspension is compressed. Scrub occurs when the end of the suspension control arm travels in a long arc and causes the wheel to move to the side as it moves up or down. This arc can be seen in the Macpherson strut design in Figure 2. Our last consideration, toe angle, is how much the wheels angle in or out while the car is driving straight. Toe angle is shown in Figure 3. Bump steer, lateral scrub and toe angle will have to be greatly considered in conjunction with the steering team to optimize efficiency and steering design. [4]

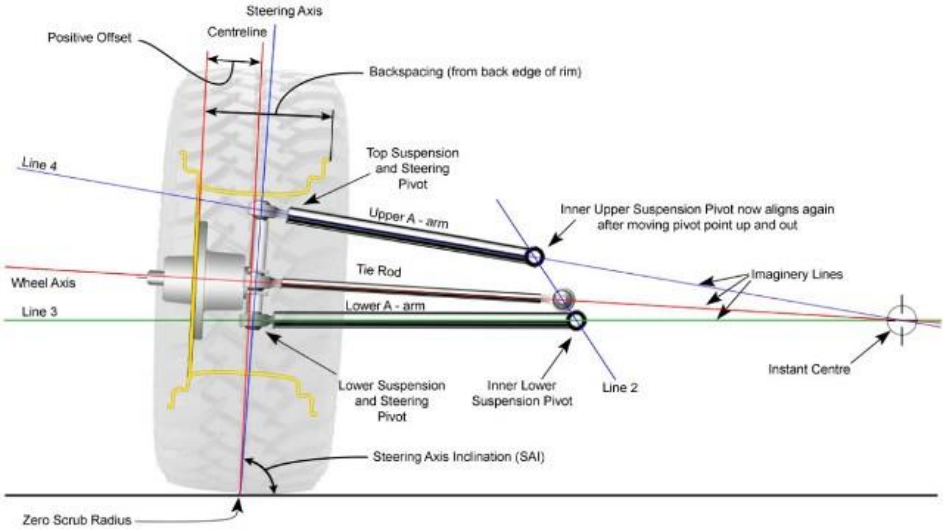

Figure 1: Bump steer diagram [6].

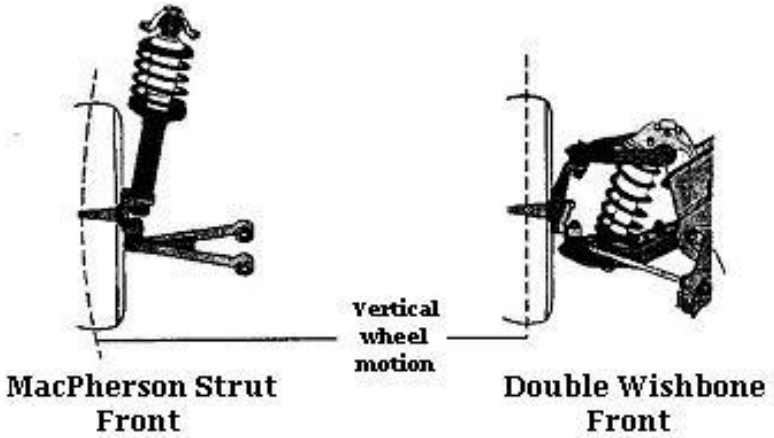

Figure 2: Example of lateral scrub [7].

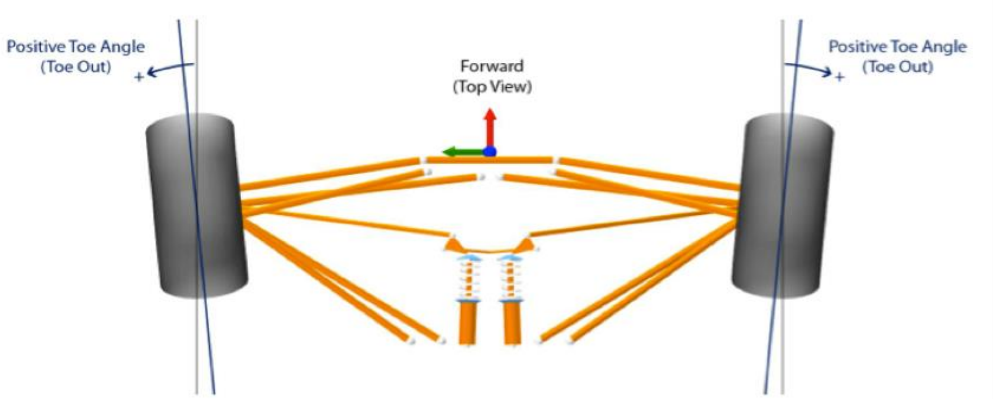

Figure 3: Example of toe angle [8]

The suspension system of any car has to be designed alongside the frame, brakes, and the steering to ensure compatibility with the entire vehicle. The steering system must be integrated into the front suspension system which limits the viable suspension options. The rear suspension does not deal with steering so the front and rear suspensions can have different designs. All four wheels must also incorporate a braking system which must be considered when designing the mounting points for the suspension.

Before choosing the style of suspension of a car, it is important to understand everything about the vehicle. The first consideration is whether the car is a unibody or the body and frame are designed separately. A unibody car has a frame built into the body of the car. This means that the body and the frame act together as the structure for the vehicle. The other option is designing them separately, in which case, the body of the car cannot act as a structural component. Some suspension systems are suited well for only one of these configurations so it is important to understand the structure of the vehicle.

Suspension systems can be designed as dependent or independent systems. A dependent suspension system moves together along with its front or rear wheel partner. In an independent suspension system, each of the four wheels can move independently from each other. The independent system is beneficial because the car can maneuver around corners and over bumps more easily than a dependent suspension system. Independent suspension is the most common style of suspension in cars. However, these systems tend to be much more expensive than dependent systems because of their complexity and the amount of extra parts they require.

Integrating steering limits us on options for the front suspension system. In our brainstorming, we came up with three main options for the front suspension. The first option is the Macpherson strut, shown in Figure 2. The Macpherson strut consists of a single control arm, a spring damper system, and struts that connect to the frame of the car. This suspension system is utilized in unibody cars because the strut runs all the way up into the frame of the car. It is hard to incorporate this system within a body on a frame style car. The benefit of this suspension system is that it is a very simple design and takes up little room in the body of the car. Because of the minimal design, it would be lightweight and relatively inexpensive to build. One downside of this system is that it takes horizontal loads very poorly. Additionally, the single control arm design limits adjustability in the geometry, making it difficult to minimize bump steer and wheel scrub. [4]

The second option for a front suspension system is the double wishbone, shown in Figure 2. The double wishbone is similar to Macpherson strut, but consists of two control arms instead of one. This design can be integrated into a frame style car and can be stronger and stiffer than a Macpherson strut. The control arms are unequal lengths and not parallel which allows the designer complete control of the suspension geometry and how the wheel travels. The downside of multiple control arms is added complexity. The double wishbone design is heavier, more expensive, and takes up more space than a Macpherson strut. [4]

A third option that we will take into consideration is a modified bicycle suspension fork. This would be completely unchartered territory because no solar car team has attempted to integrate this style of suspension into their vehicle. The bicycle fork is a telescoping shock with an integrated spring and damper. It mounts to the wheel on both sides and the steering would be easily integrated. Unfortunately, this design would be difficult to mount to the car frame and may not take lateral loads well. The bicycle fork would also be more difficult to design because it has not yet been used in a solar car. However, if we can overcome these setbacks the bicycle fork has the potential to be less expensive, lighter, and more compact than all the other designs so far [5].

The rear suspension can use any of the above suspension designs because we do not have to integrate steering. Additionally, we have the option of a trailing arm suspension. Trailing arm suspension systems use a single control arm connected to the frame with a hinge. A spring and damper connect the arm to the frame at a second point, shown in Figure 4. The trailing arm system does not handle lateral loads well and can be quite heavy if it has to be long. Conversely, trailing arm suspension is extremely simple and compact when compared to double wishbone or Macpherson strut and has no lateral scrub. [4]

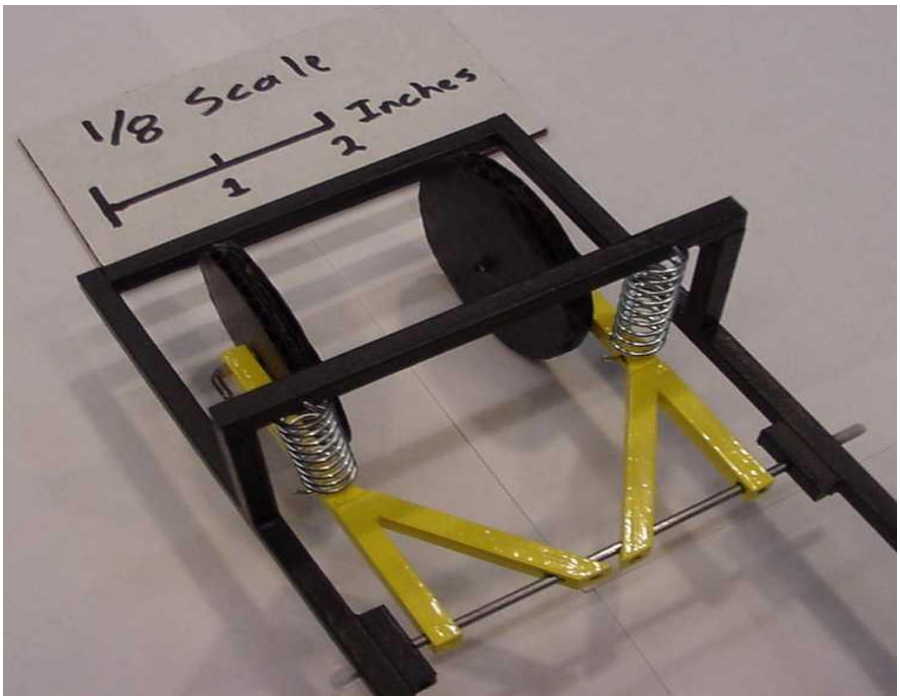

Figure 4: Model of rear trailing arm suspension [8].

3. Objectives

Our primary goal as the suspension team is to design a front and rear suspension system for a performance solar car. We have specific customer requirements and engineering specifications that we will design for which are shown in Appendix A as part of a QFD table. The QFD (Quality Function Development) was used to turn our customer needs into specific engineering requirements, and prioritize those requirements. Additionally, more information about engineering specifications is found in Table B.1 of Appendix B. We will ensure that our design is safe by analyzing all situations the solar car may endure. We will choose a shape and material that will give us a reasonable factor of safety against yield to ensure that the structure will not fail at our worst case scenarios. We will also optimize the final design to meet the structure, manufacturing and aerodynamic teams' requirements. Table 1 shows our chosen values for our initial engineering specifications.

Our first engineering specification is quick wheel removal. PROVE Lab will want to do extensive testing on the vehicle before we finalize the design and make our run at the world record. A big testing point will be changing out wheels and trying out different types of tires, so easy wheel removal will be important. Our initial goal is to remove the wheel in less than five minutes. We believe that this is a reasonable time because a car can be removed in a similar amount of time with the right equipment.

Our next specification is the weight of the suspension system. This will be a big factor in our design to reach maximum target speed. We want our total suspension weight to be less than ⅛ of the total vehicle weight. Depending on the style of the suspension, this can be achieved very easily or may not be achieved at all. If we decide to use a rear trailing arm suspension, this can add a significant amount of weight to the vehicle, whereas a double wishbone can be designed to be lighter.

Shock absorption of a suspension system is an integral part for the safety of the vehicle. One of the most important parts of the shock is the spring we choose. We are designing for speed and performance rather than comfort, so we will be choosing a stiffer spring. Race cars generally have a natural frequency of two to three Hertz [4]. Our target spring natural frequency is in the range of two to three Hertz to match that of a racecar.

Handling is not a major part of the design for our vehicle, but it cannot be neglected due to safety issues with the FIA. A dangerous aspect of the suspension and steering system is the amount of bump steer that is produced when going over a bump. Our goal is zero bump steer to maximize the safety of our vehicle. Bump steer can cause instability and unpredictability, which could ultimately result in a crash [10].

Another important design consideration is to make sure our suspension system is functional at our target speed. At higher speeds any sort of bump in the road or change in direction will increase the load imposed on our suspension. In order to make sure our system does not fail, we will design for worst load case scenarios at 70 miles per hour.

When a wheel encounters a bump, the suspension system has to take the impact of the bump and dissipate a large amount of energy. The way the wheel moves in a lateral direction over this movement is the scrub. We do not want any lateral movement in our suspension system so we will try to minimize it and ideally achieve zero lateral scrub.

One of the hardest parts of our design is going to be confining our design to fit within the aerodynamic team constraints. These will be constantly changing and we will need to adapt our design based on the design variations they show us. Currently the aerodynamics team wants the wheel fairings to be 12 inches or less in width. This narrow wheel fairing will drastically influence the shape of our suspension system.

As mentioned earlier, our suspension system must be designed for the worst-case scenario. Most likely we will never see this case because we will be attempting the world speed record on a flat airplane runway which should be free of any bumps or turns. Nevertheless, we will be designing to worst case scenarios so that we meet and exceed any and all FIA safety requirements. Our factor of safety goal is 1.5 against yield but is subject to change. We aimed for a low factor of safety because we want to limit the weight and size of the suspension.

Our last engineering specification is to minimize the static toe angle. Our goal is zero static toe angle to maximize performance and efficiency. With an inward or outward toe angle, both energy and performance would be lost due to friction and any toe angle could cause bump steer.

Table 1: Formal Engineering Specification Table (L=Low, M=Medium, H=High, T=Test, A=Analysis, S=Similarity, I=Inspection)

Spec. #	Parameter Description	Requirement or Target (units)	Tolerance	Risk	Compliance
1	Wheel removal	5 minutes	Max	L	T
2	Weight	15% of total car weight	Max	H	A, T
3	Natural Frequency	2.5 Hz	± 0.5 Hz	L	A, T, S
4	Functional Speed	70 mph	Min	L	A, T, S
5	Tire Scrub	0 inches	± .5 inches	H	A, T, S
6	Width	12”	Max	H	A, I
7	Worst Case F.O.S	1.5	Min	L	A
8	Height	30”	Min	H	A, I
9	Toe Angle	0°	± 2°	L	A, I, S

4. Design Development

In finalizing our suspension design, we considered both the type of suspension we could use and the material we could use to make it. In the selection of both we considered how they would affect the weight, cost, size, complexity, strength, safety, and efficiency of the overall system. We also looked at how well the components would fit inside an aerodynamic fairing and mate with the frame of the car and the steering system. These considerations especially contribute to passing the FIA safety test, as the FIA looks at the car as a whole in verifying its safety. After selecting carbon fiber as the superior wishbone material, we considered different methods of manufacturing carbon fiber rods and what angle of fibers we need in our rods.

4.1 Suspension Selection

Upon finishing our background research about the different types of suspension systems, we followed several steps to narrow down our selection. We started with a simple Pugh Matrix as seen in Table 2. We compared the different styles of suspensions and material to our customer requirements.

Table 2: Pugh Matrix comparing styles of suspension and material selection.

Criteria	Suspension Design					Materials	
	Standard Design	Alternatives				Standard	Alternative
	Double Wishbone	Bike Fork	MacPherson	Trailing Arm		Aluminum	Carbon Fiber
Lightweight	0	0	0	-		0	+
Cheap	0	0	+	+		0	-
Simple	0	+	+	+		0	-
Safe	0	-	-	-		0	+
Compact	0	+	+	+		0	+
Cushion Solar Parts	0	-	-	-		0	0
Efficient	0	0	-	0		0	0
Strong	0	-	-	-		0	+
Easy wheel removal	0	0	0	0		0	0
Compatibility with steering	0	0	0	NA		0	0
Compatibility with frame	0	-	-	+		0	-
Aerodynamic	0	+	0	+		0	0
Pass FIA safety test	0	-	-	-		0	0
Total	0	-1	-2	0		0	+1

In the first four columns we made the double wishbone our standard and rated everything in comparison to this suspension design. The double wishbone has zeroes in every category, meaning a neutral performance. If something else has a plus then it performed better than the double wishbone design in that category. Similarly, a minus means that the design performed worse than the double wishbone. A zero means that performance was the same as the double wishbone. According to the total scores, the double wishbone and the rear trailing arm suspension came out to be the best two options with scores of zero. The biggest advantage that the double wishbone has over the others is that it is the strongest design, while also being relatively light and extremely efficient. It has also been used extensively in other cars, which will make it easier to pass the FIA safety test. The trailing arm suspension performed admirably as well even though it can only be implemented in the rear suspension because it cannot integrate steering. The main advantage of the trailing arm is its simplicity and how well it fits into an aerodynamic fairing. However, after a few rough calculations, we found that the rear trailing arm suspension would have to be very heavy to withstand the required loads, so we decided to use a double wishbone for the whole suspension.

In addition to comparing styles of suspension, we also compared what type of material to use for the wishbones. We met with our senior project advisor, Dr. Doig, and he pushed us to consider

carbon fiber as the material for the wishbones. Most solar cars use an aluminum alloy to make their wishbones so we made aluminum our standard and compared carbon fiber to it. The comparison can be seen in Table 2. Carbon fiber is significantly stronger for the weight than aluminum, especially in axial loading which is mostly what the wishbones will experience. Carbon fiber tubes met our customer requirements and engineering specifications much better than aluminum so we are using it for our suspension wishbones. More research on carbon fiber and its manufacturing process are discussed next.

4.2 Carbon Fiber

Carbon Fiber is a thin strand of material made of mostly carbon. It is an anisotropic (direction dependent) composite with a very high specific strength. However, the specific strength of carbon fiber is dependent on how it is manufactured and the direction in which it is laid. In this report we will focus on the methods of producing carbon fiber tubing opposed to carbon fiber sheets. Carbon fiber tubing is generally manufactured by either pultrusion or roll wrapping methods. There is also a less common but valuable method called filament winding.

4.2.1 Manufacturing Carbon Fiber

Pultrusion is a continuous manufacturing process for composite materials. Fibers are reinforced with a thermosetting resin and "pulled" through a heated die for curing [11]. The main advantage of pultrusion is that it is a versatile process that allows for intricate shapes to be made with custom dies. Although pultrusion has great shape versatility, it is unidirectional meaning all the fibers lay along the axis of the tube [12]. Unidirectional carbon fiber is strong in one direction and only that direction. A photo of Pultruded carbon fiber is seen in Figure 5.

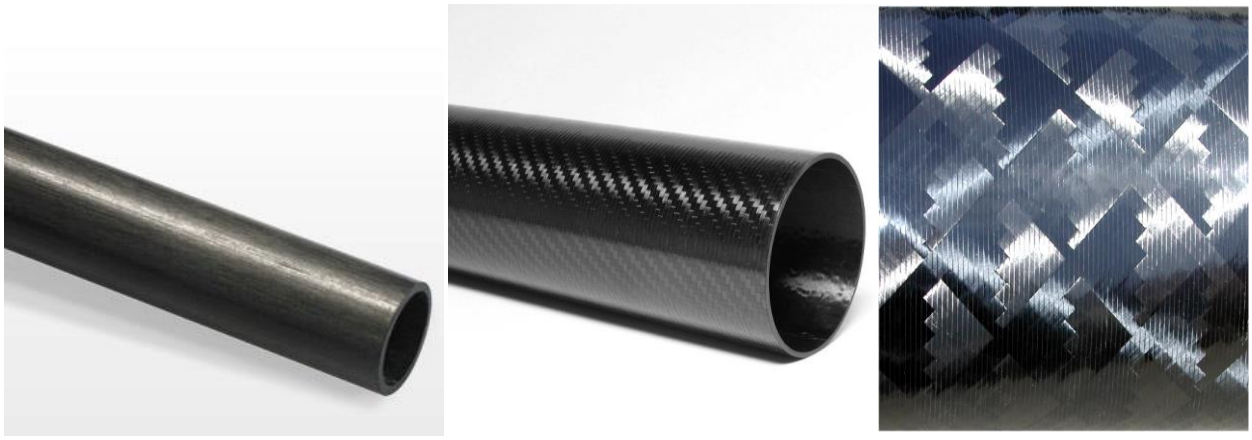

Figure 5: Pultruded (Left) [13], Roll Wrapped (Middle) [14], Filament Wound (Right) [15]

Roll wrapping carbon fiber involves applying a resin to pre-impregnated composite carbon fiber cloth. Pre-impregnated (pre-preg) cloth comes with a matrix material (such as epoxy) already embedded into the carbon fiber cloth [16]. Because the cloth is pre-impregnated, material properties of the carbon fiber provided by companies tends to be much more consistent [16]. The carbon fiber cloth is then "wrapped" around a shaft in a spiral fashion with a consolidation tape under tension to hold the cloth in place while it cures [16]. Multiple layers of carbon fiber cloth are added to achieve the desired tube thickness. Carbon Fiber cloth can be purchased with many

As described before, pultrusion is a manufacturing method for carbon fiber that is unidirectional. The fibers can only be laid at 0° along the axis of the tube. The compressive and tensile strengths of pultruded carbon fiber are similar to that of steel. However, because pultruded carbon fiber is unidirectional it has very poor mechanical properties in torsional and shear loading. This limits the applications for pultruded carbon fiber.

Roll wrapped carbon fiber can have several layers of carbon fiber cloth. An example of a roll wrapped carbon fiber tube with multiple layers is seen in Figure 7. These layers of cloth can have several different fiber angles to account for the different loading cases. There are two common forms of carbon fiber cloth that can be purchased. The first is the 0°/90° orientation. The fibers are weaved together at 0° and 90°. This orientation is great for tensile, compressive, or radial load cases. The other commonly sold carbon fiber cloth is weaved together at 45°/-45°. This configuration handles torsional loading very well, but has poor axial strength. Combining different fiber angles in the lay-up of your carbon fiber strengthens the tube in each direction and results in a "more" isotropic style material.

Filament wound carbon fiber is wound by a programmed robot, which gives the designer freedom in choosing carbon fiber angle. The robot can be programmed to change fiber angles whenever desired. Roll wrapped tubes and filament wound tubes have similar mechanical properties if the same fiber angles are used in the manufacturing process.

4.3 Best Method for Our Suspension

	6	2	7	10	10	7	7	49	
	12%	4%	14%	20%	20%	14%	14%	100%	
Option	Material Cost	Torsional Strength	Shear Strength	Tensile Strength	Compressive Strength	Ease of Purchase	Specific Stiffness	Score	
Roll Wrapped 0/90	3	2	2	5	5	4	4	4	IIII
Roll Wrapped 45/-45	3	5	4	1	1	4	4	3	II
Pultrusion	4	1	1	4	5	4	2	3	III
Filament Winding	3	4	4	4	4	3	5	4	IIII

Table 3: Decision Matrix for Carbon Fiber Manufacturing Method

We determined that our main loads on our carbon fiber tubes would be bending, shear and minimal torsion with an emphasis on bending. To account for these load cases we are considering incorporating a combination of 0° and ±45° fiber angles. In addition to these angles, we also wanted to incorporate a 90° fiber angle to protect against any hoop stresses that might form at the connection points at the end of our tubes. The type of loading the rods will experience is reflected by the first row of numbers in our decision matrix (Table 3). Those numbers represent the relative importance of each design consideration. Each type of carbon fiber is rated on a scale of one to five (with five being the best) on its performance in each design consideration. The decision matrix resulted in a tie between filament wound and roll wrapped carbon fiber tubing. Manufacturers tend to use either of these processes because they both yield similar mechanical properties if the same fiber angles are used in the process. For our suspension we can use either of these methods to obtain our desired result. We ultimately decided to use roll wrapped tubing because it is cheaper and easier to buy.

4.4 Connection Points

4.4.1 Aluminum Inserts

The next step for our suspension system was designing the connection points for our suspension. Because we plan on purchasing our carbon fiber tubing, we have to design custom inserts that connect the tubes. Examples of the top and bottom insert connections are shown in Figure 8. We are planning on using a high strength aluminum alloy such as 6061-T6 or 7075-T6 to maximize our strength at the joints of our suspension. Another alternative we thought about was to use a welded steel joint, but this adds significant weight and complexity over machined aluminum joints. A downside to aluminum is that it is not easily epoxied to carbon fiber, but we feel the benefits of aluminum outweigh this problem, especially if we hire a company to do the epoxy for us.

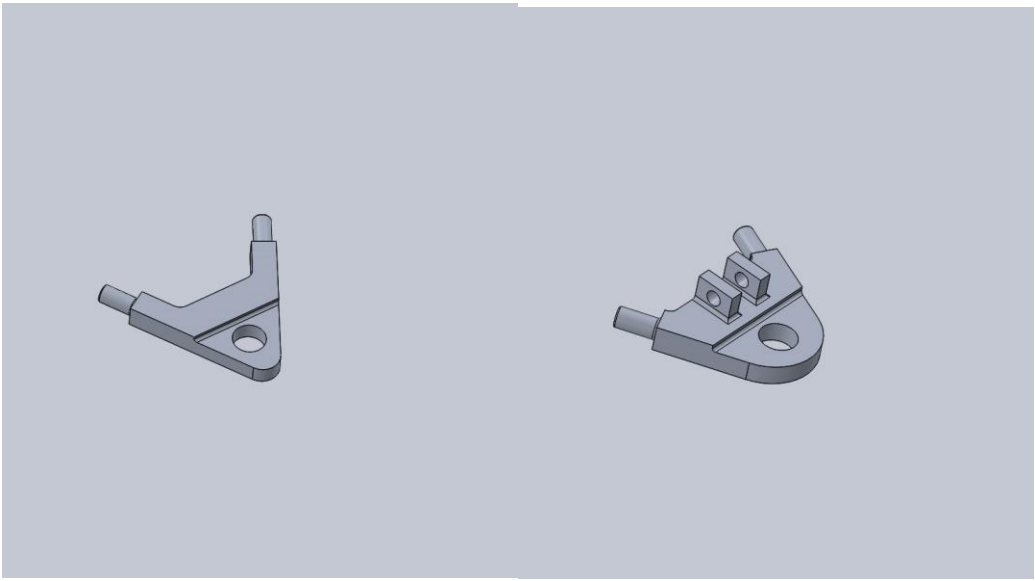

Figure 8: Top A-Arm Insert (Left) and Bottom A-arm insert (Right)

4.4.2 Rod Ends and Inserts

To attach the carbon fiber rods to the brackets on the frame we will use rod ends. Rod ends are mechanical joints that have a ball swivel with a hole at the end. The hole allows for a bolt to go through and keep the ball swivel vertical. These joints allow the ball swivel end to attach to the frame of the car and the other end to rotate up and down with the suspension. An example of a rod end can be seen in Figure 9. To attach the rod end to the carbon tube, we will epoxy a steel female insert into the tube, into which we can then thread the rod end. This gives us the added advantage of being able to fine tune the suspension geometry by screwing in or out the rod end.

Figure 9: Male Rod End (Left) [19] and Female Insert (Right) [20]

4.4.3 Frame Integration

The last concern we had is how the rod ends will connect to the frame. The frame that the suspension connects to will be made from carbon fiber and it will contain a honeycomb-nomex core. The combination of carbon fiber with honeycomb-nomex allows for a lightweight structure. The downside of this structure is its ability to handle compression loading. Our first design for the wishbone frame connection is shown in Figure 10. The brackets are located at the corners of the frame, which allows the force to be transmitted between two walls. After meeting with representatives from Tesla, we gained insight into strengthening the wishbone frame connections. Steel backing plates will be put behind the carbon fiber structure as seen in Figure 11. The plates will add minimal weight to the overall design and are necessary to prevent fracturing of the frame.

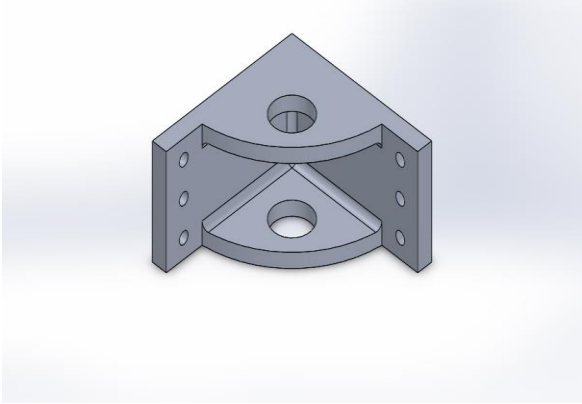

Figure 10: Wishbone Connection

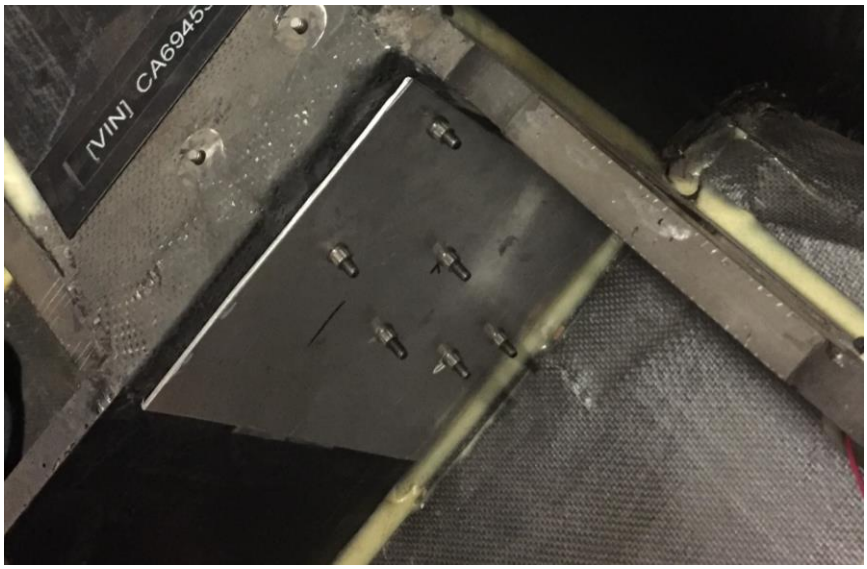

Figure 11: Steel Reinforcement backing plate from Stanford's solar car.

4.5 Upright Design

The upright of our suspension system was designed to raise the car further from the ground. The aerodynamics team determined that raising the car base further from the ground mitigates ground effects, reducing drag.

The first idea we had was to use a bike-fork for our upright. Using an existing bike fork allows us to simplify our design and focus more on the exact suspension geometry. We looked at aluminum and carbon fiber bike forks. Both carbon fiber and aluminum bike forks weighed less than two pounds. However after some simple analysis it was determined that a bike fork would not be strong enough to handle the sideways load of a four wheeled vehicle. For safety reasons we determined that a bike fork would not work in our design.

The next idea we had was to machine a fork-shaped upright out of aluminum. Using aluminum would allow us to make an upright tailored to our design. Making the upright out of aluminum would also decrease the amount of custom parts that we would need because the connection points could be machined into the upright. The downside of this option is the cost. A large amount of aluminum is needed to create the upright that we need. We spoke to Dan Waldorf, a manufacturing professor at Cal Poly and he said that it would cost about two thousand dollars in aluminum and labor to create each upright. Another downside to machining a one-piece aluminum upright is the extra wasted material. To save some money we looked into making a two piece upright. Because we are limited on money and the suspension is not a crucial part of the overall solar car design, we determined that machining custom uprights was not in our budget.

The next option we looked into was welding steel tubing to make our upright. We spoke with John Fabijanic, a professor at Cal Poly who has designed suspension systems and worked on formula cars about the best option for our suspension. He confirmed that steel tubing would be the best option for our uprights. Steel tubing is relatively inexpensive and can be welded easily. We first looked into using circular tubing, but after attempting to design the connection points to the wishbones we decided it would be best if we used rectangular tubing. Rectangular tubing is

similarly priced and it would be much easier to integrate the connection points that connect the inserts to the upright. After researching the different steel alloys, we decided that chromoly 4130 was our best option because of its high yield strength.

We will have to machine aluminum brackets to connect the upright to the wishbones. The top and bottom brackets will be different lengths to create an offset wishbone geometry while allowing the wishbone pivots to all sit in the corners of the frame.

Table 4: Final Design Decisions

Design Consideration	Final Decision
Suspension Type	Double Wishbone
Carbon Fiber Manufacturing Method	Roll Wrapped
Wishbone Joints	Custom aluminum inserts
Carbon Fiber Rod Joints	Male rod ends with female inserts
Wishbone to Frame Joints	Custom aluminum brackets
Upright Design	Steel, bike fork shape
Upright to Wishbone Joints	Custom aluminum brackets

5. Final Design

5.1 Initial Design

Figure 12 shows our initial suspension design for the front and back of the car. The changes we had to make later on will be later in this section. This design involves a welded steel upright with bolted on machined aluminum brackets. These brackets interface with the aluminum wishbone joints via a spherical bearing and clevis pin, allowing the upright to turn as well as move up and down. The aluminum wishbone joints are epoxied into carbon fiber tubes which have threaded inserts with high misalignment rod ends epoxied into the opposite ends. The rod ends are attached with clevis pins to brackets that are bolted into the corners of the car frame. The shock is mounted with a pin and bushing to the bottom wishbone joint. The top of the shock is attached with a custom aluminum bracket to a part of the frame that will extend out to accommodate the shock placement.

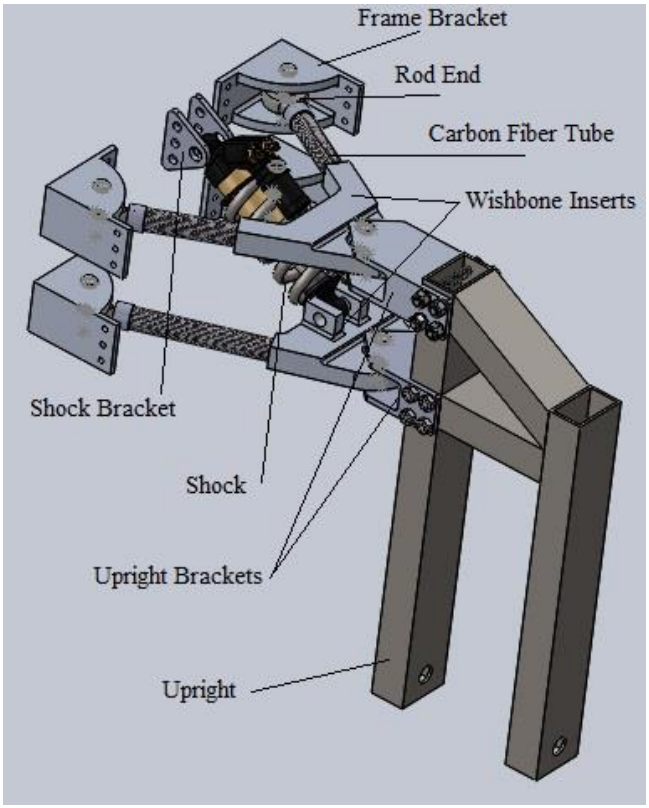

Figure 12: Final Suspension Design

We designed our suspension system to withstand our worst-case scenario of sliding sideways on an asphalt road. We took a static analysis approach because most of the loads are constant and we designed against yield. Although unlikely, this approach ensures that our suspension system will not fail under normal loading conditions. Because our car is designed to drive straight on a smooth road, we did not perform a fatigue analysis. We also assumed a kinetic coefficient of friction of .80 which is at the higher end of the range.

5.1.1 Upright

The upright is to be made of chromoly 4130 steel because of its high yield strength. Our worst case scenario is when the car is sliding sideways. The upright is suspended high off the ground which creates a high bending moment as seen in Appendix E. To properly carry this load with a reasonable factor of safety, steel is the most efficient option. Our total approximate weight of the upright is around 33 pounds which is much less than 15 % of the total weight of the car (one of our original design specifications).

5.1.2 Upright Brackets

The connection points attach to the upright and the aluminum inserts. They will be made from 6061-T6 Aluminum. They will be CNC machined in house because of their simple geometry. The connection points will be secured to the uprights with 4 high strength steel bolts. The top connection will be slightly longer than the bottom connection to create a kingpin angle. Having a kingpin angle minimizes the amount of horizontal scrub seen by the tire when the suspension compresses and retracts. The aluminum connections and their finalized dimensions can be seen in Appendix B.

5.1.3 Carbon Fiber Tube Selection

Traditionally, the wishbones of a suspension systems are made from either steel or aluminum. Our car is made mostly of carbon fiber and weighs significantly less than a normal car, so our loading conditions are also significantly less than that of a normal car. The wishbones in our suspension act as two force members in axial loading. Because of our simple loading case, a thin carbon fiber tube can be used to satisfy the loads with a large factor of safety.

A load line analysis is used to determine the fewest number of plies of roll wrapped carbon fiber needed to successfully carry the applied load. Complex loading conditions can be simplified by analyzing each load separately to determine how many plies are required in that direction. This method ignores the fact that each layer of carbon actually works together to carry the applied load. By ignoring this fact, it is actually an overestimated value, which provides a small factor of safety to the design.

Fiber angle orientation is important when purchasing tubing. Because we have a simple tension and compression loading case, we technically only need fibers in the 0-degree direction. However, it is also beneficial to have an outer ply of carbon fiber in the 90-degree direction. This layer protects the carbon fiber from debris that could damage the tubes. We spoke with Dr. Mello, a composites teacher at Cal Poly and he recommended buying our tubing from Rockwest Composites. After emailing them and telling them about our overall project, they agreed to give us 10% off our total order. Another benefit of ordering our tubing from Rockwest Composites is that they provide the desired lay-up orientation for each style of tubing. An example of a carbon fiber tube lay-up provided by Rockwest Composites can be seen below in Table 5.

Table 5: Rockwest Composites Example Layup

Ply #	Orientation	Location
1	0	Inside

2	0	
3	90	
4	90	
5	0/90	Outside

5.1.4 Aluminum Insert

The inserts connect the A-arms and the uprights. The bottom and top insert will be different because the bottom insert will hold the shock. The inserts are to be made of Aluminum 6061-T6 because of its high specific strength and machinability. The aluminum inserts will be CNC machined in house because they have relatively simple geometry. The inserts will also hold Aurora high misalignment swivel bearings to allow the upright to move freely. The swivel bearings will be press fit into the aluminum inserts. Clevis Pins will go through the misalignment holes as seen in the assembly drawing in Appendix B.

5.1.5 Rod Ends and Steel Inserts

Right hand 5/8-18 super swivel rod ends are to be purchased from McMaster Carr. These rod ends have a ball swivel of 65 degrees so they can misalign up to 32.5 degrees in each direction. The radial load rating for the super swivel rod ends is over 10,000 lbs. Our load of approximately 1900 pounds is much less than the rated load, so we have a fairly high factor of safety with regards to our rod ends. A picture of our chosen rod ends can be seen in Appendix D. Each rod end will be connected with a matching right hand 5/8-18 steel insert that will be purchased from QA1, a suspension company. The steel insert will then be epoxied into the ends of the carbon fiber tubing using an aluminum-carbon epoxy. The steel inserts and their specifications can be seen in Appendix D.

5.1.6 Frame Brackets

The last custom part that we designed is our corner connection points that connect the rod ends to the frame of the car. The connections are to be made of aluminum 6061-T6. They will be CNC machined in house because they have simple geometry. All four connections will connect in the corners of the carbon fiber car frame to distribute the load more evenly. The connection points will be bolted with four high strength steel bolts through the carbon fiber car frame. The steel bolts that we selected have an ultimate tensile strength of 150,000 psi and are to be purchased from McMaster Carr.

5.2 Shock Selection and Mounting

Our main criteria in selecting a shock was to find one that fit inside our size constraints, provided a natural frequency of around 2.5 Hz, allowed for three inches of travel, and held a quarter of the car's weight. The Cane Creek DBair shock fulfills all of these needs, and allows us to fine tune the rebound, damping, and spring rate relatively easily. Our car only travels in a straight line, so it is not necessary to have all the adjustability that this shock offers, but this adjustability does guarantee that we can have the desired ride characteristics with very little extra design work.

In mounting the shock, we aimed for a roughly linear motion ratio throughout the shock stroke length that would allow the wheel to move three inches within the shock's two-inch stroke length. To calculate these values we modelled the system in Lotus Shark, a suspension kinematics

software made by Lotus. Additionally, the shock had to fit in the carbon fairing, which stops us from using a conventional shock mount. Some solar cars use a pull rod and bell crank linkage so that the shock can lay horizontal to fit in the fairing easier. We considered this at first, but when we modelled the bell crank and a direct mount design in Lotus Shark, we saw no reason to make a pull rod style linkage. Mounting the shock directly to the lower wishbone and the frame near the upper wishbone brackets fit much easier into the fairing and frame. Furthermore, this design has a linear motion ratio and uses about 1.6 inches of shock stroke for three inches of wheel travel, seen in Figure 14. In the figure the vertical axis shows how much the shock is compressed, while the horizontal axis shows how much the wheel moves. Because of the simplicity and favorable performance characteristics we decided to direct mount our shocks to the lower wishbone as shown in Figure 13.

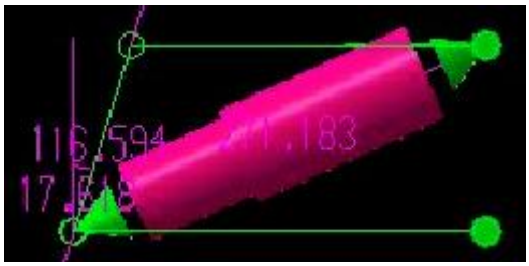

Figure 13: Direct Mount Model in Lotus Shark

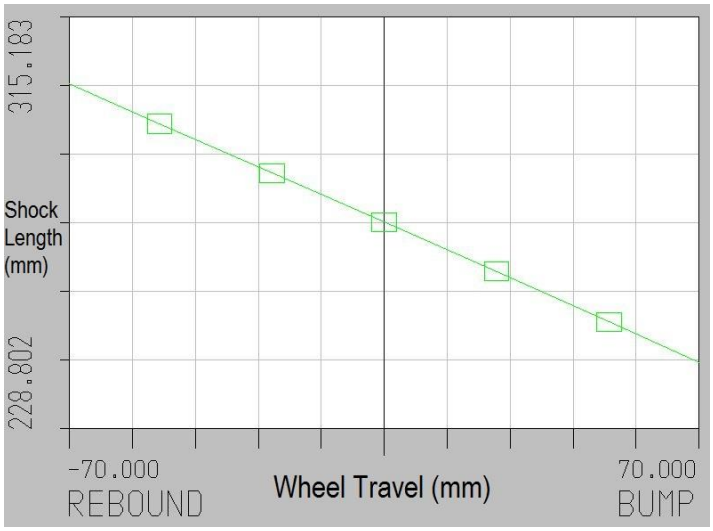

Figure 14: Shock Length vs Wheel Travel

5.3 Geometry and Kinematics

The geometry and kinematics of the suspension were modelled and designed by Adam using Lotus Shark software. This software allowed us to build a 3D model of the suspension and view a huge variety of motion parameters. Adam built a model of our preliminary suspension design in Lotus Shark using the dimensions required by the aerodynamics team and then adjusted the dimensions that we had control over to optimize certain suspension characteristics. Specifically, we looked at minimizing bump steer and scrub. These both make the car significantly less efficient and potentially dangerous to drive. Once these values were minimized, we designed in a five degree caster angle and tried to minimize camber change through the travel of the suspension. Adding a small caster angle encourages the wheels to track in a straight line and

stabilizes the steering. Camber does not matter for handling purposes, but if we had an excessive amount the wheel could rub on the carbon fiber fairing. We also designed for close to zero scrub radius, which helps to further minimize bump steer.

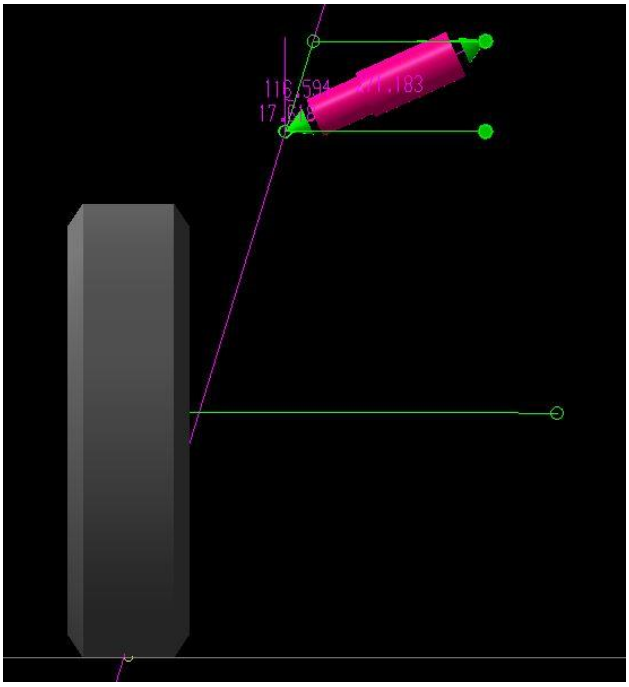

Figure 15: Lotus Shark Suspension Model

In the Lotus Shark model, we were able to design a suspension geometry that exceeded our original expectations. The model is shown in Figure 15. Table 6 summarizes the results of our design. Graphs of the suspension motion parameters are provided in Appendix E.

Table 6: Suspension Geometry Parameters

Caster Angle	5°
Scrub Radius	0°
Scrub	< 0.1 Inches
Bump Steer	~ 0.2°
Kingpin Angle	17.07°
Static Toe Angle	0°
Static Camber Angle	0°
Camber Change	< 2°

5.4 Final Design

Unfortunately, the design described in section 5.1 was not used for our final design because of late changes made by the aerodynamics team. In order to reach our goal of 70 miles per hour, they needed to decrease the width of the wheel fairing by a significant amount. After narrowing the fairing, there was not enough space for our initial design. We did a complete redesign, simplifying our design while making it safer. The new design is seen in Figures 16 and 17. We are now using this design for the front suspension only. A complete rear suspension redesign will be done later, but is outside the scope of this project.

Figure 16: Final Suspension Model

Figure 17: Completed Suspension Build in Plywood Display Mount

5.4.1 Final Upright Design

The new upright (Figure 18) is made of 6061-T6 aluminum and weighs roughly three pounds. It supports the wheel on just one side while our old upright had supported both sides of the wheel. The one-sided design greatly reduces the width of the wheel attachment to fit in the narrower wheel fairings. The upright is solid through the body, which makes it much stronger than the steel upright while maintaining a similar weight. We also reduced the number of stress concentrations in our new design because it no longer requires welding or notching.

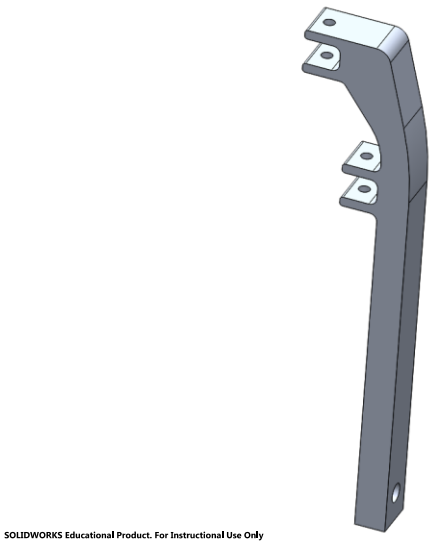

Figure 18: Final Upright Model

5.4.2 Final A-Arm Design

Another change we had to make was to the horizontal width of the A-arms. This dimension is shown below in Figure 19. The chassis width where the A-arms attach has to be greater than the width of the wheel so that the wheel can sit between chassis panels. The A-arms in our original design were too narrow so in order to house the full wheel, we needed to increase the A-arm width to 25 inches. To accomplish this width adjustment, we made the angle between the carbon rods larger and lengthened the carbon rods, keeping the overall length of the A-arms the same. As a result, we made the adjustment without any decrease in strength or change to the kinematic properties of the system.

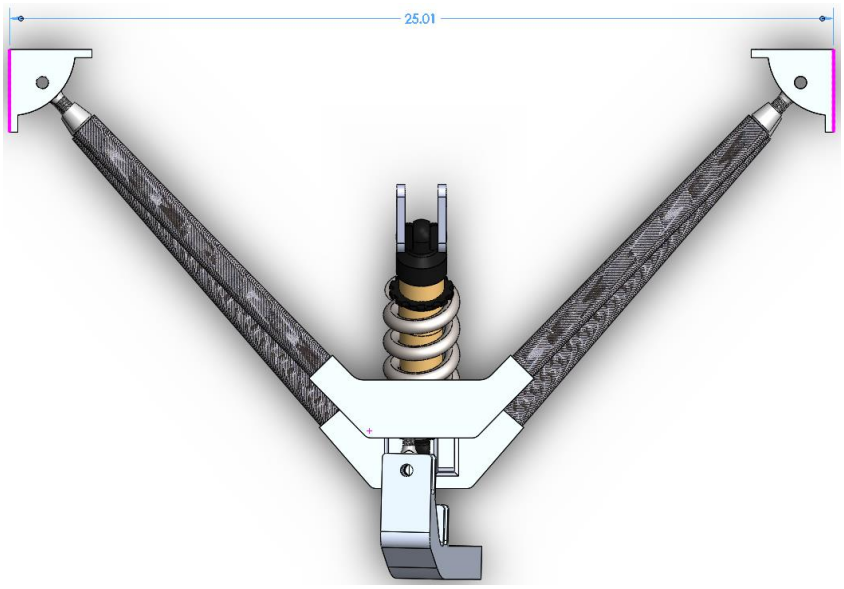

Figure 19: Horizontal A-Arm Dimension

5.4.3 Final Top and Bottom Insert Design and Rod Ends

The top and bottom inserts changed slightly with our new design. We chose to use rod ends to connect the upright to the inserts instead of spherical bearings. The rod ends are threaded into the holes in the inserts as seen below. With rod ends the caster angle in our upright is achieved more easily than with spherical bearings. Additionally, in threading the inserts into the uprights, we could adjust the suspension geometry for fine tuning on the car. We initially worried about putting rod ends in bending, but determined it was not a problem after further analysis. We also had to round corners of the shock tabs on the bottom insert to accommodate a shock.

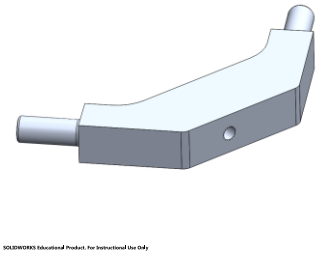

Figure 20: Top Insert

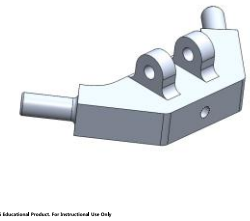

Figure 21: Bottom Insert

We also changed the size and threading of the rod ends. The previous design called for 5/8”-18 right hand threaded rod ends but we determined that 3/8”-24 rod ends were strong enough. By switching rod ends, we were able to use smaller tube ends and smaller carbon fiber tubes. By reducing the size of these three features, we saved a good portion of money and some weight.

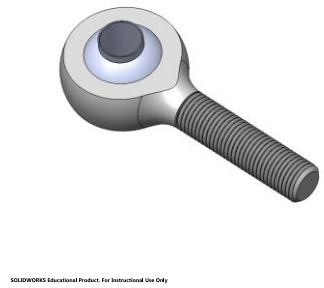

Figure 22: Rod End

5.4.4 Carbon Tubes and Tube Ends

Our original design had carbon tubes with only 0° and 90° plies. Even though we theoretically only need plies in these two directions, we decided to add plies in the 45° and -45° directions for added strength. It’s hard to predict exactly what type of loading conditions will be imposed on our suspension, and these extra plies will account for any conditions that we did not expect. The new carbon fiber tubes have 17 plies including 0°, 90°, 45°, and -45°.

In addition to adding extra plies and different ply angles we reduced the inner diameter of our carbon tubes. Adding more plies increased the tube wall thickness and allowed us to use narrower tubes while achieving the same safety factor as before the change.

SKU : 45558-HM Rev A		
Ply #	Orientation	Location
1	0	Inside
2	0	
3	0	
4	45	
5	-45	
6	0	
7	0	
8	90	
9	90	↓
10	0	
11	0	
12	-45	
13	45	
14	0	
15	0	
16	0	
17	0/90	Outside

Figure 23: The Ply Structure of Our Carbon Fiber Tubes

We also had to change the tube ends from our previous design because we changed the rod end and carbon fiber tube sizes. The new tube ends have a smaller inner and outer diameter with no notable change in strength for the system.

Figure 24: Tube End

5.4.5 Corner Brackets

The corner brackets changed only slightly. We thickened the walls on the corner brackets to account for potentially higher loading than we originally expected. We also increased the size of the six holes on the side to allow for bigger bolts. There were a few minor changes added for ease of manufacturing that will be discussed in the manufacturing portion of this report.

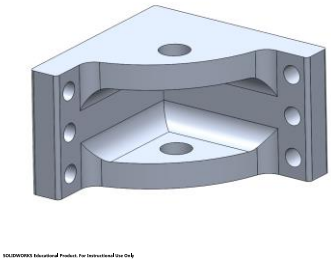

Figure 25: Corner Bracket

6. Design Verification Plan

From our FMEA (Appendix F), we determined that the most critical mode of failure is going to be at any of the epoxied joints. Failure here would cause complete destruction of the suspension system and possibly damage to the car or injury to the driver. Furthermore, we do not have a good way of predicting how the bond will behave without testing, making this a very dangerous part of the design. To account for this we are going to use the tensile tester to test the strength of the epoxy bond to aluminum and steel. In order to run this test we need to purchase carbon fiber samples and steel and aluminum shafts that can be epoxied into the carbon fiber tube. First we will try using the epoxy and making the bond ourselves. If we cannot make a strong enough bond then we will outsource to a composites company and have the bonding done professionally.

The second test we will run before building is the verification of the suspension geometry. We will build a model of the suspension out of PVC pipe, wood, rod ends, and spherical bearings, as well as a model of the frame out of wood. We will assemble everything and measure the motion of the suspension to make sure that it is consistent with the computer model. When the suspension is fully built we will weight it, calculate its natural frequency, time the wheel removal,

and test its functional speed. Our DVP (Design Verification Plan) is included as Figure 16 for reference.

ME428 DVP&R Format

Report Date: 5/3/2016			Sponsor: PROVE Lab		Component/Assembly: Suspension			REPORTING ENGINEER: Adam O'Camb				
TEST PLAN								**TEST REPORT**				
Item No	Specification or Clause Reference	Test Description	Acceptance Criteria	Test Responsibility	Test Stage	SAMPLES		TIMING		TEST RESULTS			NOTES
						Quantity	Type	Start date	Finish date	Test Result	Quantity Pass	Quantity Fail	
1	Epoxy Strength	Tensile Test	Withstand 2000 lbs	Alex Power	DV	4	B	5/10/2016	5/17/2016				
2	Suspension Geometry	Prototype and Measure	Minimal bump steer and scrub	Adam O'Camb	DV	1	B	5/10/2016	5/17/2016				
3	Wheel Removal	Time wheel removal when upright is made	Less than 5 minutes	Adam O'Camb	PV	1	C	6/10/2016	7/1/2016				
4	Weight	Weigh when whole thing is assembled	Less than 15% of car weight	Adam O'Camb	PV	1	C	6/10/2016	7/1/2016				
5	Natural Frequency	Measure with accelerometers when suspension is assembled	Approximately 2.5 Hz	Alex Power	PV	1	C	6/10/2016	7/1/2016				
6	Functional Speed	Test when car is assembled	Car must be able to go 70 mph	Alex Power	PV	1	C	6/10/2016	7/1/2016				

Figure 26: DVP

7. Manufacturing

7.1 CNC Machining

7.1.1 Uprights

The uprights of the suspension required four individual set-ups to complete. Because the uprights are 17 inches long, two vices were required to secure the metal stock in place while machining. The maximum vertical travel of the HAAS mill that Alex used was 20.8 inches, which was too short to hold the upright vertical and fit the drill bit above it. The top hole was located using a center drill in the mill and then a drill press was used to drill the hole. Furthermore, the bottom hole of the upright was just as complicated. It required a 3/8 diameter 15-inch-long drill bit because the bottom part of the upright was in the way of the tool holder. The 15-inch drill bit required very careful operation to accurately locate the holes.

7.1.2 Top Inserts

The top aluminum inserts of the suspension required five set ups to machine. The circular connection points where the carbon fiber tubes attach were the most difficult to machine. They required the use of a dial indicator and fine adjustments in the vice to ensure those parts of the upright were perfectly vertical.

7.1.3 Bottom Inserts

The bottom aluminum inserts were the most complex and time-consuming parts to machine. These parts required nine individual set-ups on the three-axis HAAS VF-2 mills. Similarly to the top aluminum inserts, a dial indicator was used in order to accurately machine the carbon fiber tube connection points. When the part was finished, we found that a shock would interfere with the corners on our bottom insert's shock tabs. To fix this we machined down the corners to a radius of ½" to avoid collision between the tabs and shock.

7.1.4 Corner Connections

The corner connections (eight total) required four individual set ups for each part. On the previous design iteration, we had different fillet radii on several features of our corner connections. We added rounded corners and increased the fillet radii for ease of machining as well as a faster run time on the parts.

7.1.5 Future Manufacturing

Manufacturing of the suspension took a significant amount of time due to the constraints of our manufacturing knowledge. Several steps can be taken in order to save manufacturing time and improve accuracy of our machined parts.

Future machining of this design could be done on a CNC mill that has five-axis capability. Some of the features were very difficult and time consuming to machine on a three-axis mill. A five-axis machine would significantly reduce set up and machining time for the top and bottom inserts. In addition to reducing time and saving money, the accuracy of the parts would increase because of the reduced number of set-ups needed. Each set up introduces a new error to a part. Reducing the number of set-ups by using a higher axis mill would be necessary in mass-producing our suspension system.

Carbide mills should also be purchased in order to machine the suspension parts much quicker. Carbide mills can machine at a speed of 1500 feet per minute while a standard high-speed steel mill can only cut at 300 feet per minute.

7.2 Bonded Parts

7.2.1 Carbon Fiber

The carbon Fiber tubes were cut using a tile saw in machine shop at Cal Poly. We the epoxied the aluminum and carbon fiber parts together in a clean and safe environment in the PROVE lab, located in Building 7 (ATL) at Cal Poly.

7.2.2 Epoxy Process

Bonding carbon fiber to aluminum is normally a very complicated process because when electrically connected to carbon fiber aluminum will immediately begin corroding and ruin the strength of the bond. To combat this, most aluminum is acid etched before bonding to carbon fiber. Because we did not feel we had the qualifications to safely acid etch our parts, Adam researched alternative ways to achieve reliable bonds without the use of acids. We found that West Systems G/flex epoxy can create a strong bond between carbon fiber and aluminum while acting as an insulator to prevent corrosion. [21] The only surface preparation required is scuffing with 80-grit sandpaper and acetone cleaning. After scuffing and cleaning the bond surfaces, we mixed the epoxy and added .007 inch diameter glass beads to control the bond gap. We slid the parts together, removed excess epoxy, and let the parts sit on a level surface in a cool, dry room to cure for 24 hours.

Prior to bonding our suspension parts, we conducted two ASME Lap Joint Shear Strength Tests with carbon fiber and aluminum samples to verify that the bond would behave as expected. This test will be further explained in the testing portion of this report.

8. Further Analysis and Testing

8.1 FEA Analysis

The analysis for our suspension was very complex and hard to model accurately. Alex was able to do a simplified finite element analysis on the bottom wishbone of the suspension system to further investigate the stresses in our suspension. Several simplifications were put in place in order to limit computation time in Abaqus. The main focus of the analysis was to see how the carbon fiber reacted under a 3-G bump load.

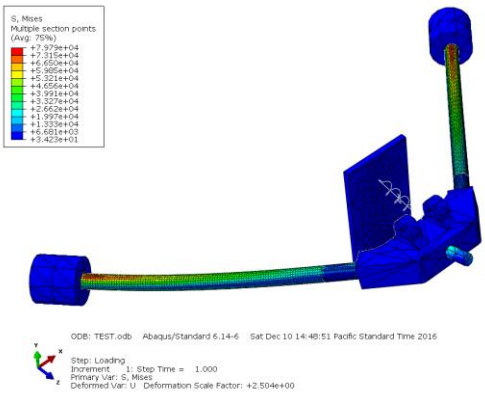

Figure 27: FEA Analysis

The conclusion of the FEA model was that we had plenty of strength along the 0-direction of the composite tubes. Rockwest composites provided their tubes with an ultimate strength much greater than 100 ksi. The highest stresses in our tubes shouldn't exceed 75 ksi as seen below in Figure: 28.

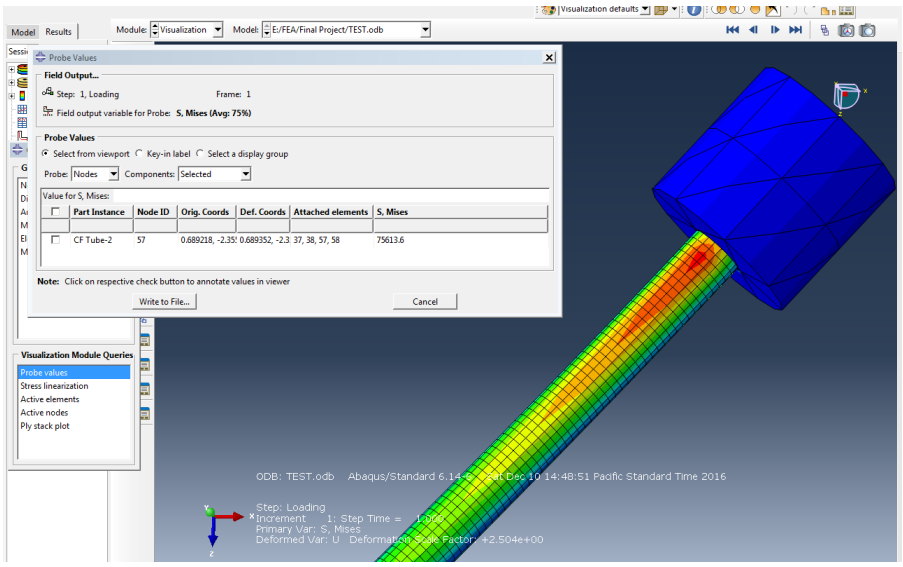

Figure 28: FEA Results

8.2 Testing

We are not yet able to do proper suspension tests and tuning because the solar car is still being manufactured. However, we did an ASME Shear Strength Lap Joint Test to verify the strength of the West Systems G/flex epoxy. We conducted two identical tests with identical results. We bonded one carbon fiber sample and one aluminum sample, both about four inches long by one inch wide. We had a bond area of one square inch and a bond gap of about 0.008. We put each sample in a tensile tester that slowly pulled the samples apart. Both tests showed no deformation in the epoxy, but the aluminum part started to yield around 2000 psi. The result of our tests is that the epoxy is significantly stronger than we need it to be.

After assembling the suspension system, we used basic measurement tools to verify that the system has the same kinematic properties as the Lotus Shark model. The dimensions are exactly the same as our models, and the horizontal scrub is 0.25 inches—not exactly the same as the model, but well within our predetermined tolerances.

We plan to do another tensile test for each A-arm to confirm that our epoxy bonds are as strong as they were in the lap joint tests. When the car is built, we will tune the shock for maximum efficiency.

Appendix A – QFD

Correlations	
Positive	+
Negative	−
No Correlation	

Relationships	
Strong	●
Moderate	○
Weak	▽

ction of Improveme	
Maximize	▲
Target	◇
Minimize	▼

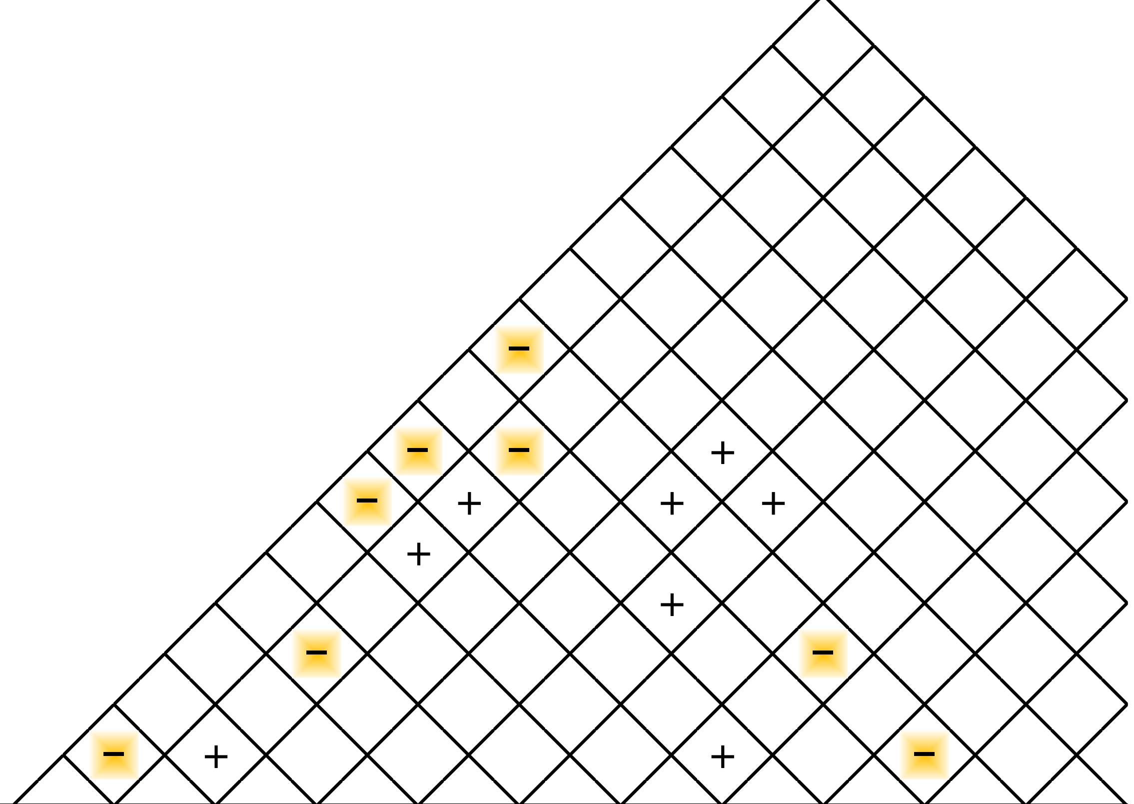

							Column #	1	2	3	4	5	6	7	8	9	10	11						
	WHO: Customers						Direction of Improvement	◇	▼	◇	▼	◇	▼	▼	◇	◇	◇	▼	NOW: Current Product Assesment - Customer Requirements					
Row #	Weight Chart	Relative Weight	Dr. Doig	Interdisciplinary Team	Manufacturing	Maximum Relationshi	WHAT: Customer Requirements (explicit & implicit) / HOW: Engineering Specifications	Quick wheel removal	Minimize total suspensi	Efficient Spring	Limit bump steer	Functional at max Spee	Minimize scrub	Minimize Number of Pa	Fit into narrow wheel fa	Withstand worst case s	Fit into tall wheel fairin	Minimize static toe angl	Our Current Product	Rear Trailing Arm	Double Wishbone	Mcpherson Strut	Bike Shock Suspension	Row #
1		7%	9	4	1	9	Lightweight	▽	●	▽		○		●	○	●	▽		0	3	2	3	4	1
2		8%	8	8	1	9	Cheap	▽	○	○	▽	○	▽	●	▽	○	▽		0	4	2	3	5	2
3		14%	6	7	8	9	Simple	●	●	○	○	▽	○	●	○	▽	○		0	5	2	4	4	3
4		9%	9	9	1	9	Safety of vehicle		▽	▽	○	●	▽			●	○	▽	0	5	5	5	5	4
5		7%	6	9	1	9	Compact	▽	▽	▽	▽	▽	▽	●	●	▽	●		0	4	2	3	4	5
6		7%	9	9	0	9	Keeps solar parts safe		▽	○	○	●	▽			●	▽	▽	0	5	5	5	5	6
7		7%	9	9	0	9	Efficient	○	●	●	●	●	●	▽	▽		○	●	0	4	5	3	3	7
8		13%	9	9	5	9	Strong		●	○		○		○		●			0	4	4	4	4	8
9		8%	2	6	4	9	Easy wheel removal	●	▽					▽	▽		▽		0	3	3	3	3	9
10		11%	5	8	5	9	Compatibility with steering	▽			●	●	●	▽	●		●	●	0	0	5	5	4	10
11		10%	5	6	5	9	Compatability with frame		○			●		○	○	▽	○		0	4	3	3	2	11
12		0%				9	Aerodynamic					●		▽	●		●		0	3	3	3	5	12

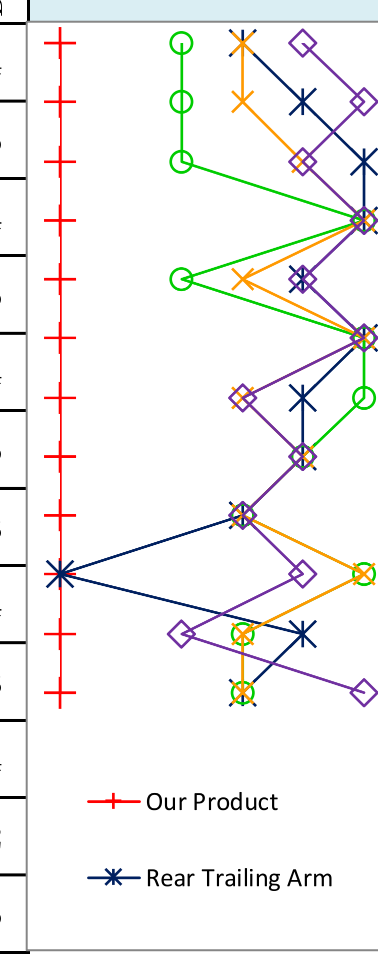

	1	2	3	4	5	6	7	8	9	10	11
HOW MUCH: Target	Change the wheel in 5 minutes	Have total suspension weight less than 1/8 of the	Have a natural frequency between 2 and 3 Hz	Tie Rod and Steering Linkage at same angle	Max Speed of 65 mph	No side wheel movement	Zero custom parts for rear suspension	Limit width of fairing to 12 inches	F.O.S. of 1.5	30 inches off the ground	Zero static toe angle
Max Relationship	9	9	9	9	9	9	9	9	9	9	9
Technical Importance Rating	248.36	451.33	215.56	268.57	499.6	236.55	413.47	275.74	373	310.65	179.66
Relative Weight	7%	13%	6%	8%	14%	7%	12%	8%	11%	9%	5%
Weight Chart											
Trailing Arm Suspension	5	3	5	5	3	5	4	5	5	0	5
Double Wishbone	5	3	5	5	4	4	1	3	3	5	5
Macpherson Strut	5	4	5	4	4	3	3	4	4	5	5
Bike Shock Suspension	4	4	4	5	3	5	4	4	4	3	4

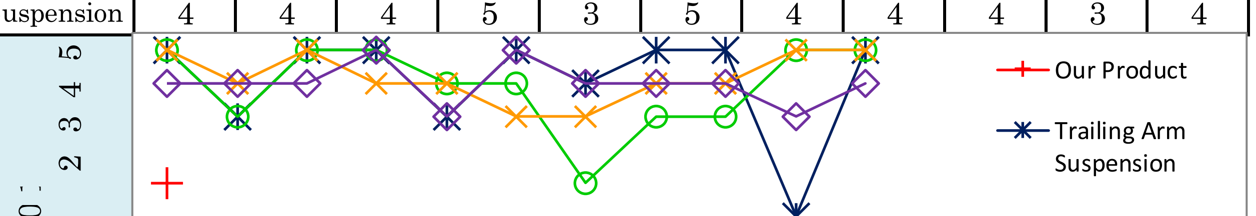

Column #	1	2	3	4	5	6	7	8	9	10	11

Appendix B – Drawings

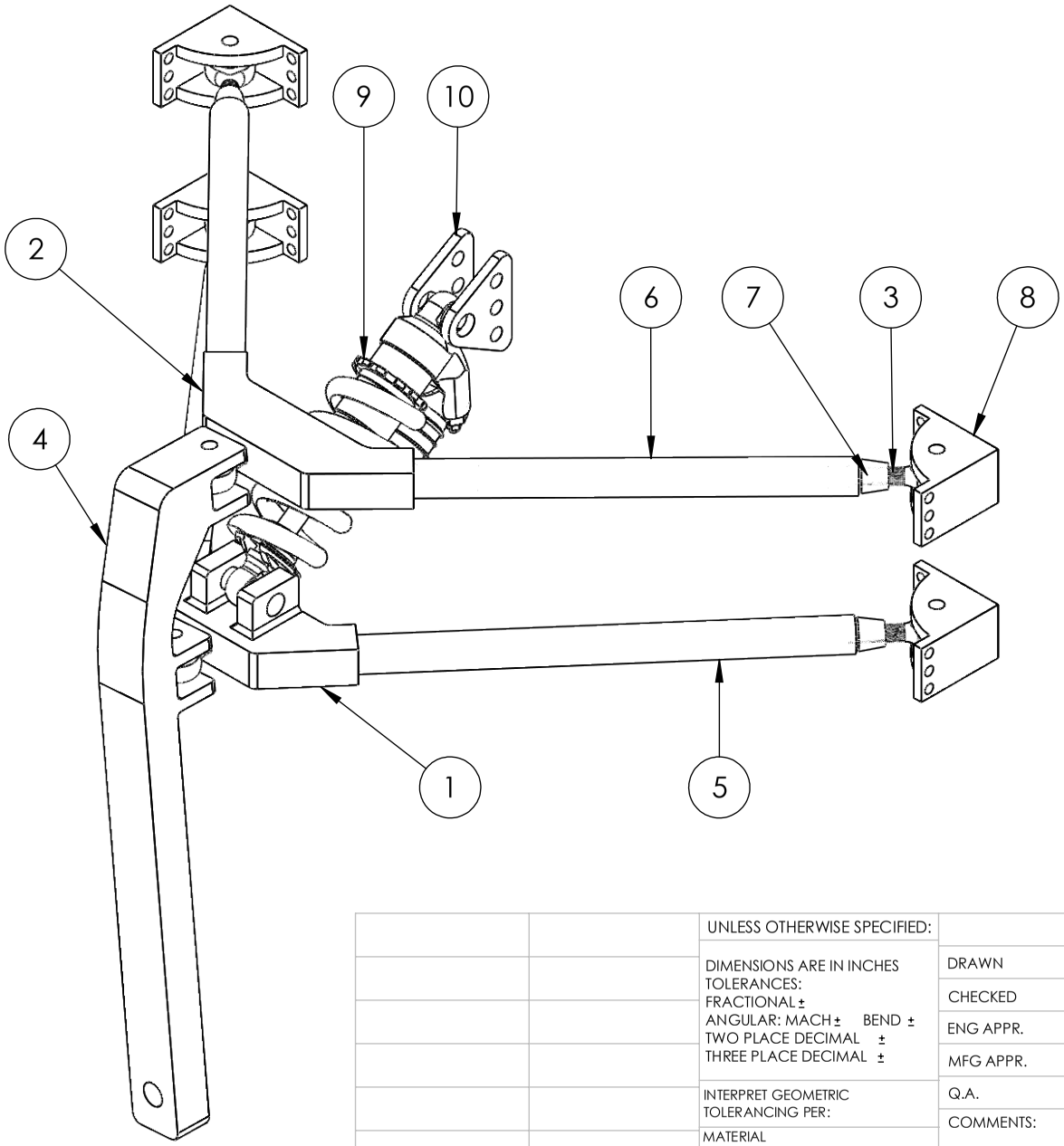

ITEM NO.	DESCRIPTION	QTY.
1	BOTTOM ALUMINUM INSERT	1
2	TOP ALUMINUM INSERT	1
3	ROD END	6
4	UPRIGHT	1
5	LONG CARBON TUBE	2
6	SHORT CARBON TUBE	2
7	TUBE END	4
8	CORNER BRACKETS	4
9	CANE CREEK DB SHOCK	1
10	SHOCK BRACKET	2

		UNLESS OTHERWISE SPECIFIED:		NAME	DATE
		DIMENSIONS ARE IN INCHES TOLERANCES: FRACTIONAL ± ANGULAR: MACH ± BEND ± TWO PLACE DECIMAL ± THREE PLACE DECIMAL ±	DRAWN	AO	12-12-16
			CHECKED		
			ENG APPR.		
			MFG APPR.		
		INTERPRET GEOMETRIC TOLERANCING PER:	Q.A.		
		MATERIAL	COMMENTS:		
NEXT ASSY	USED ON	FINISH			
APPLICATION		DO NOT SCALE DRAWING			

TITLE: SUSPENSION ASSEMBLY

SIZE	DWG. NO.	REV
A		B

SCALE: 1:8 | SHEET 1 OF 1

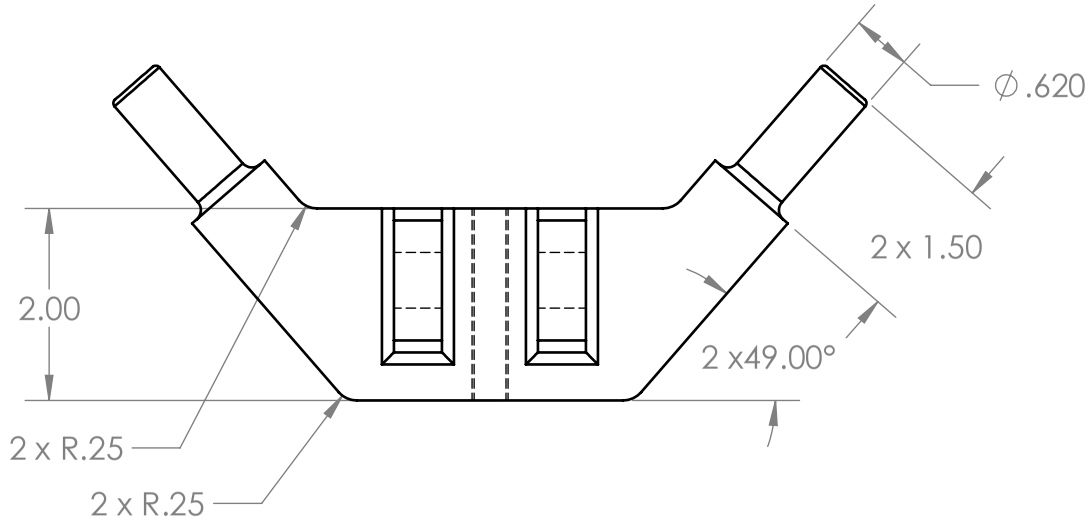

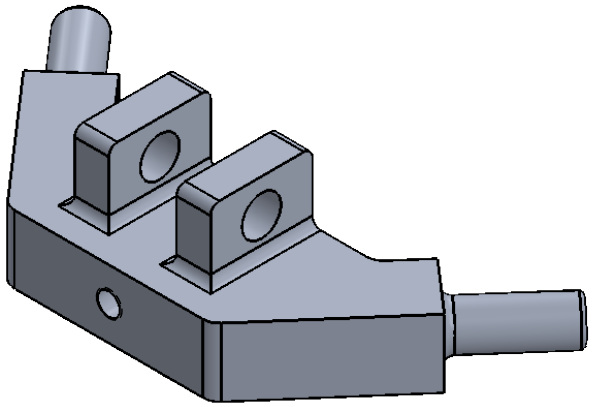

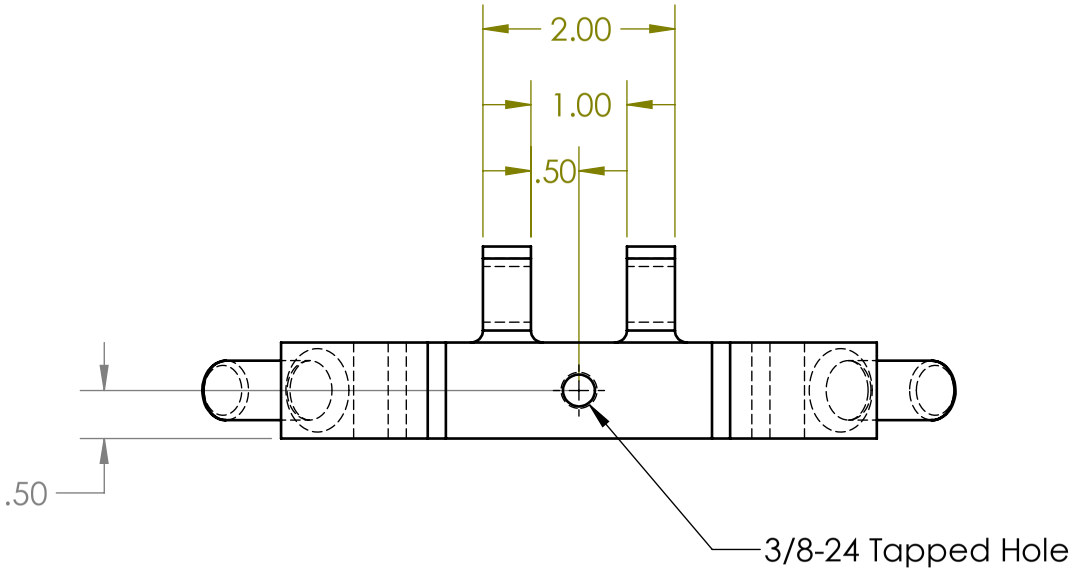

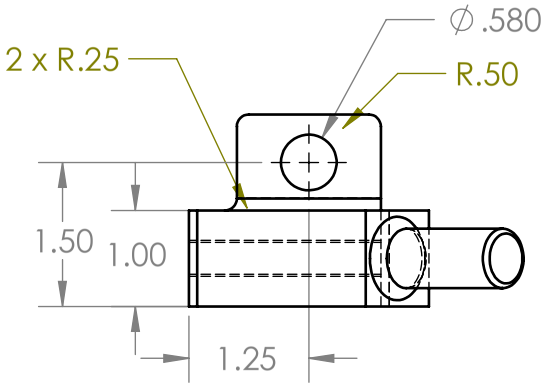

Cal Poly Mechanical Engineering SENIOR PROJECT	SOLIDWORKS Educational Product. For Instructional Use Only.		Title: BOTTOM INSERT		ALEX POWER / ADAM O'CAMB
			Date:	Scale: 1:1	

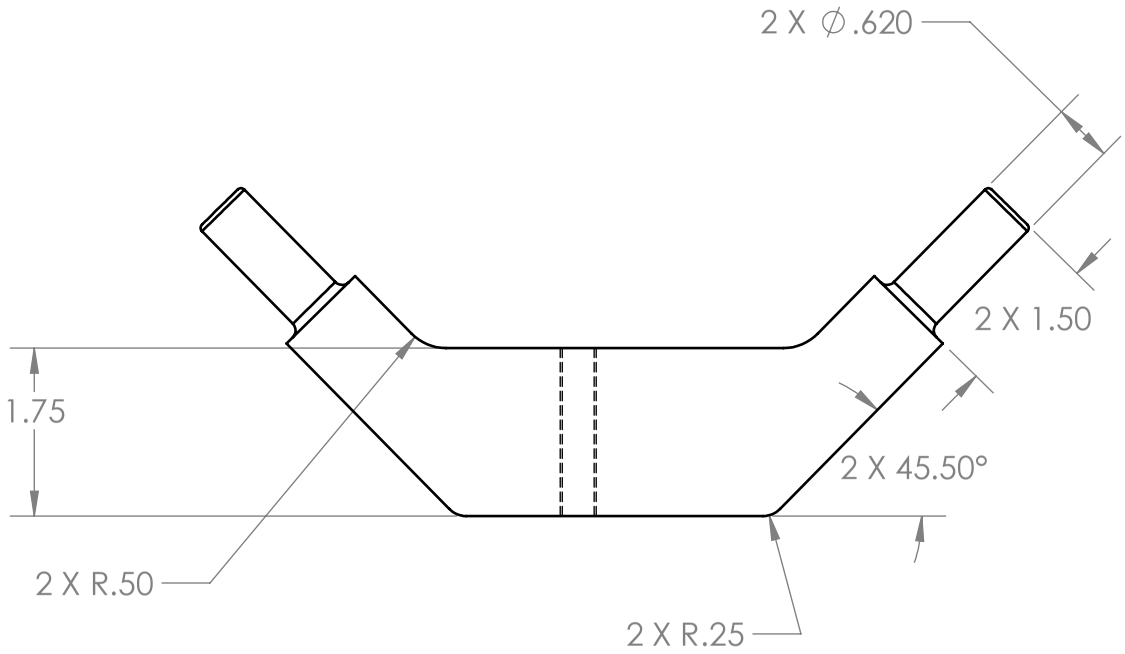

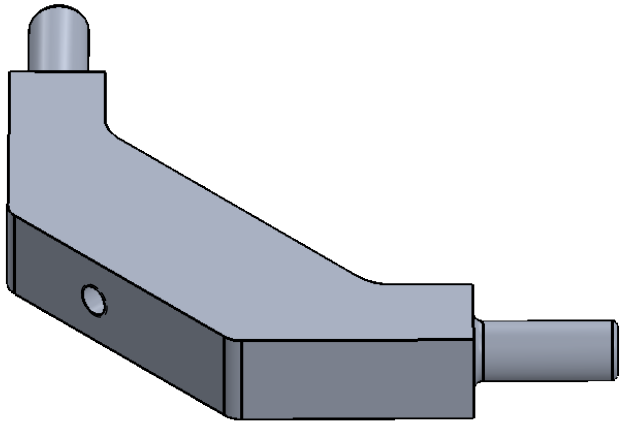

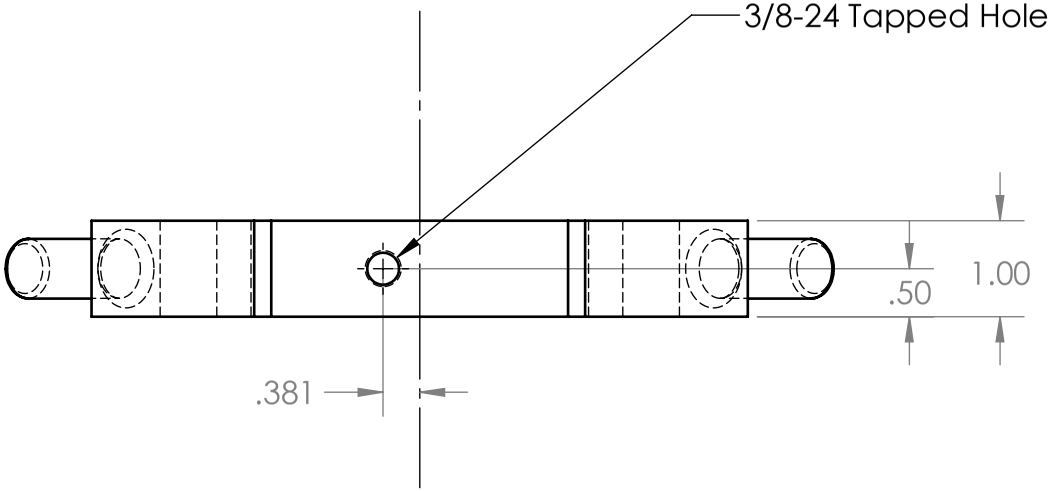

Cal Poly Mechanical Engineering SENIOR PROJECT	SOLIDWORKS Educational Product. For Instructional Use Only.		Title: TOP INSERT		ALEX POWER / ADAM O'CAMB
			Date:	Scale:1:1	

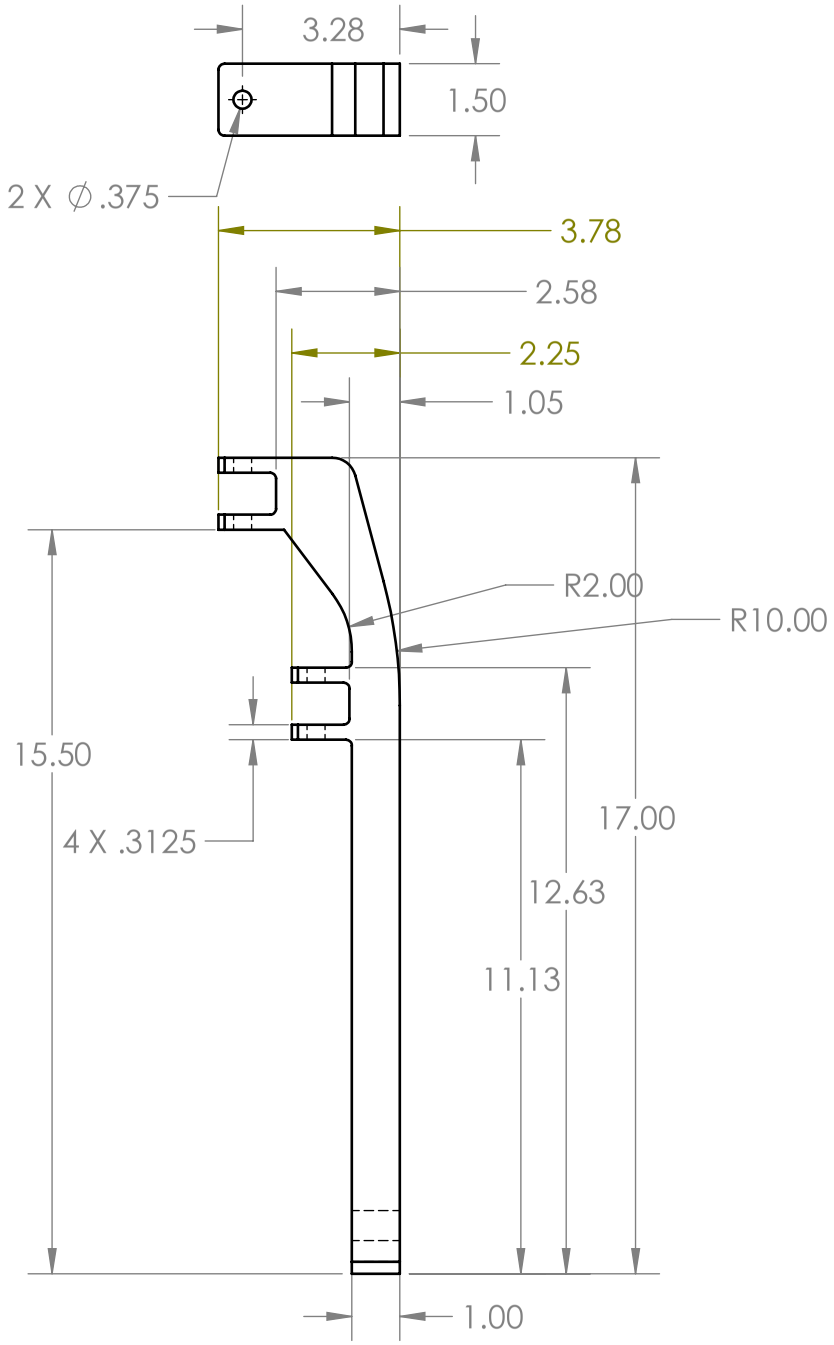

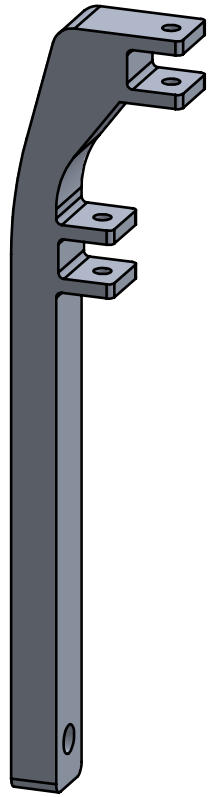

Cal Poly Mechanical Engineering SENIOR PROJECT	SOLIDWORKS Educational Product. For Instructional Use Only.		Title: UPRIGHT		ALEX POWER / ADAM O'CAMB
			Date:	Scale:	

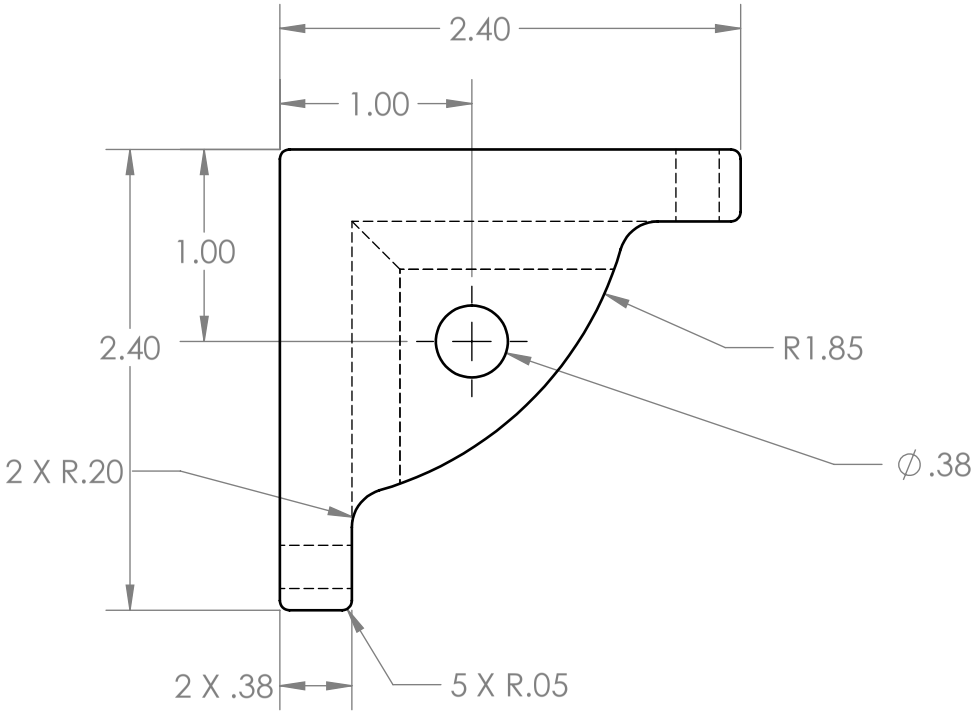

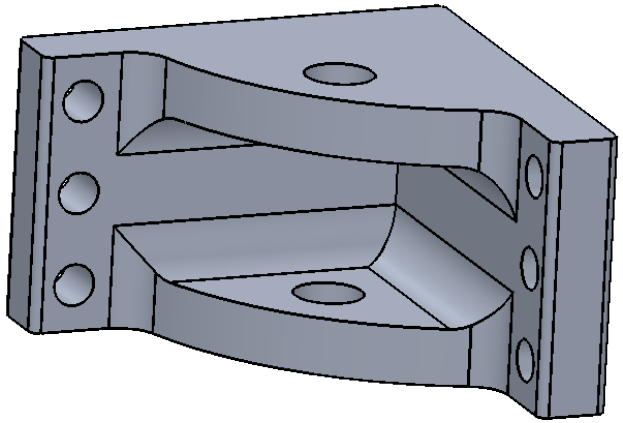

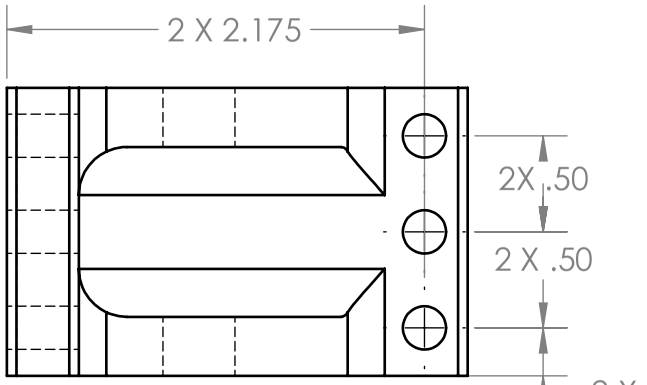

SYMMETRIC

Cal Poly Mechanical Engineering SENIOR PROJECT	SOLIDWORKS Educational Product. For Instructional Use Only.		Title: CORNER BRACKET		ALEX POWER / ADAM O'CAMB
			Date:	Scale: 1:1	

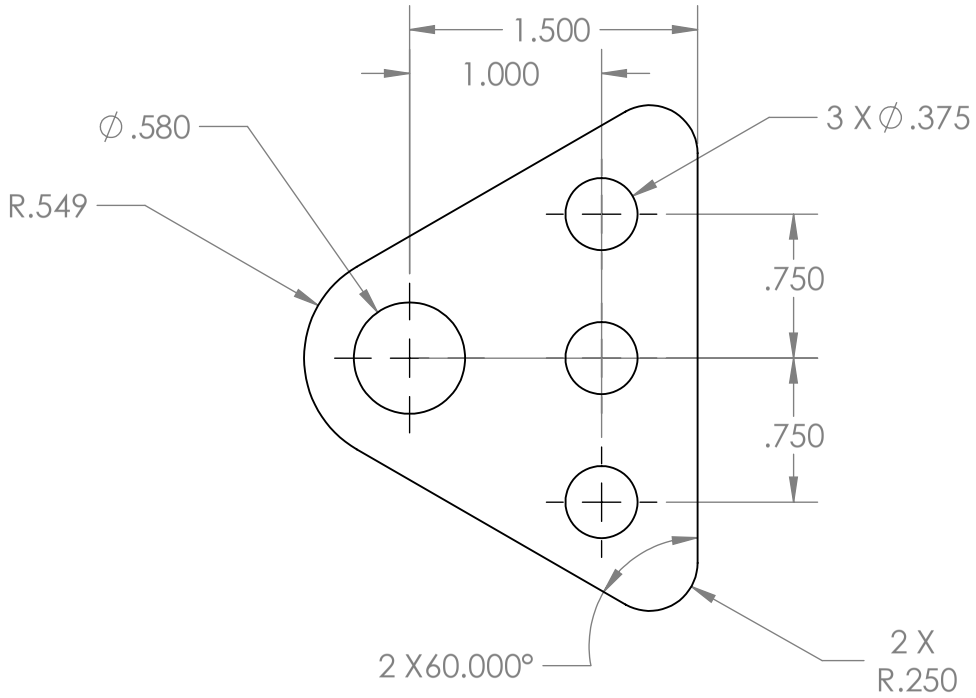

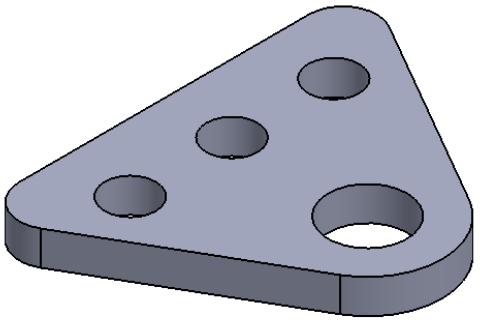

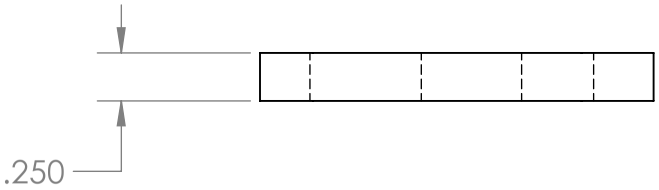

NOTES:

MATERIAL:

6061-T6 ALUMINUM

		UNLESS OTHERWISE SPECIFIED:		NAME	DATE
		DIMENSIONS ARE IN INCHES TOLERANCES: FRACTIONAL ± ANGULAR: MACH ± BEND ± TWO PLACE DECIMAL ± THREE PLACE DECIMAL ±	DRAWN		
			CHECKED		
			ENG APPR.		
			MFG APPR.		
		INTERPRET GEOMETRIC TOLERANCING PER:	Q.A.		
		MATERIAL	COMMENTS:		
NEXT ASSY	USED ON	FINISH			
APPLICATION		DO NOT SCALE DRAWING			

TITLE: SHOCK BRACKET

SIZE	DWG. NO.	REV
A	4	

SCALE: 1:1	WEIGHT:	SHEET 1 OF 1

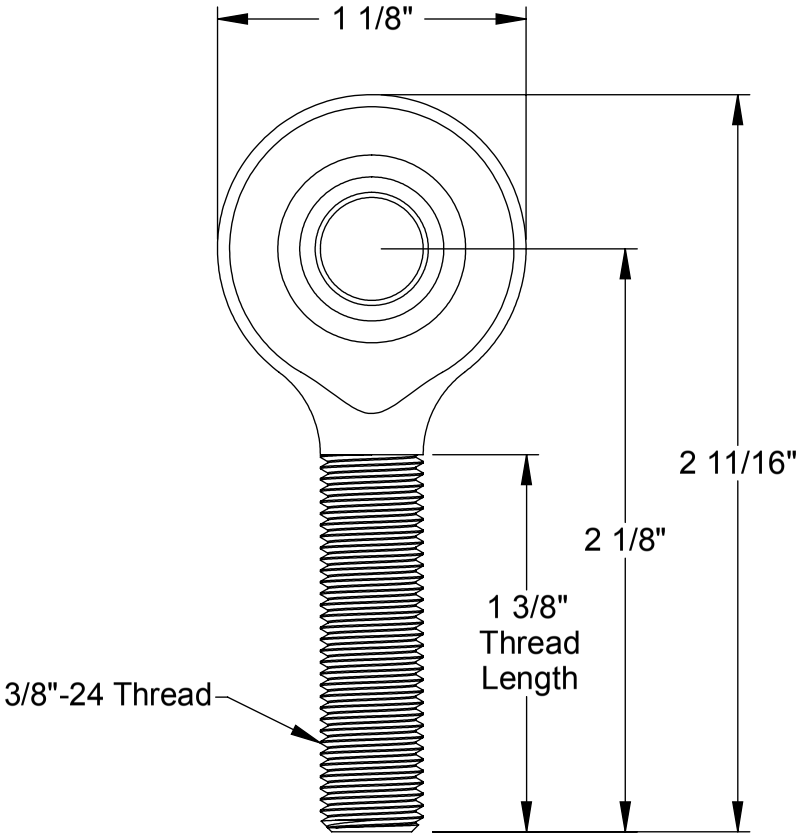

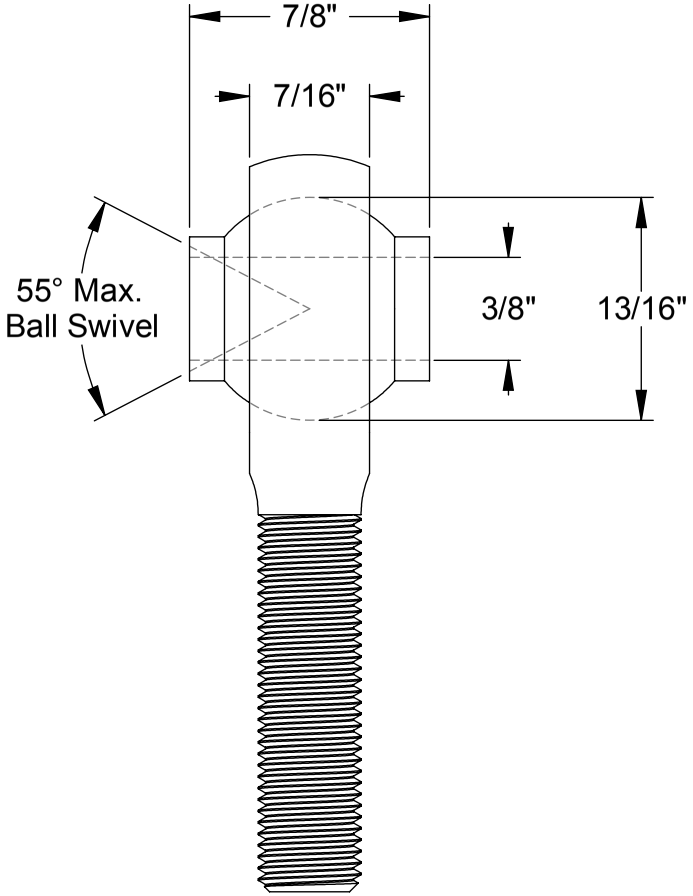

Notes: Heat Treated, Black-Oxide Coated, Alloy Steel Housing
Heat Treated, Chrome-Plated Bearing Steel Ball
PTFE Liner

McMASTER-CARR® CAD

http://www.mcmaster.com

Information in this drawing is provided for reference only.

PART NUMBER **6960T61**

Right-Hand Thread
Ball Joint Rod End

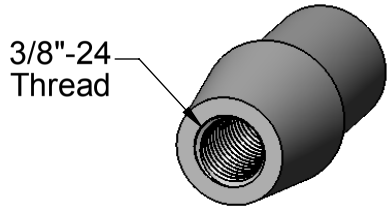

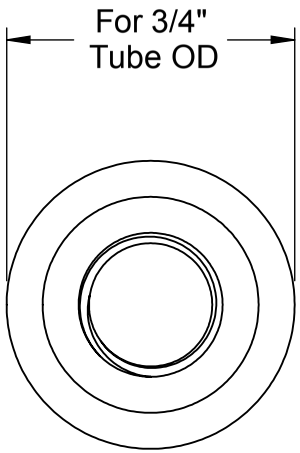

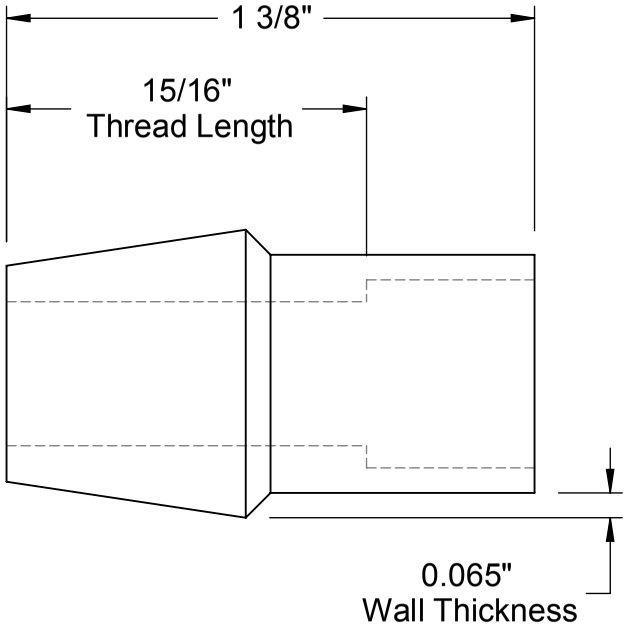

McMASTER-CARR® CAD http://www.mcmaster.com 	PART NUMBER **94640A115** Tube-End Right-Hand Threaded Weld Nut

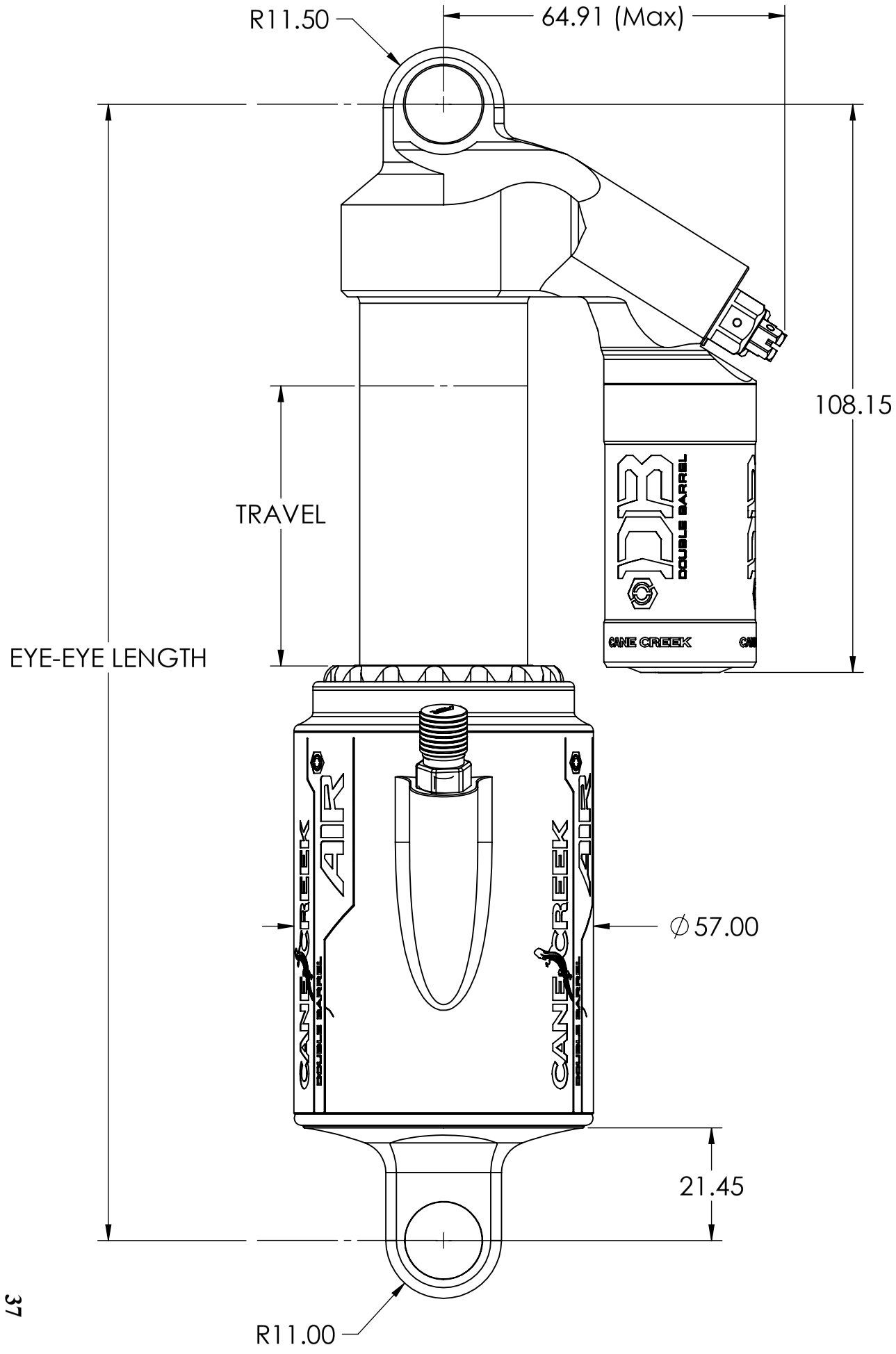

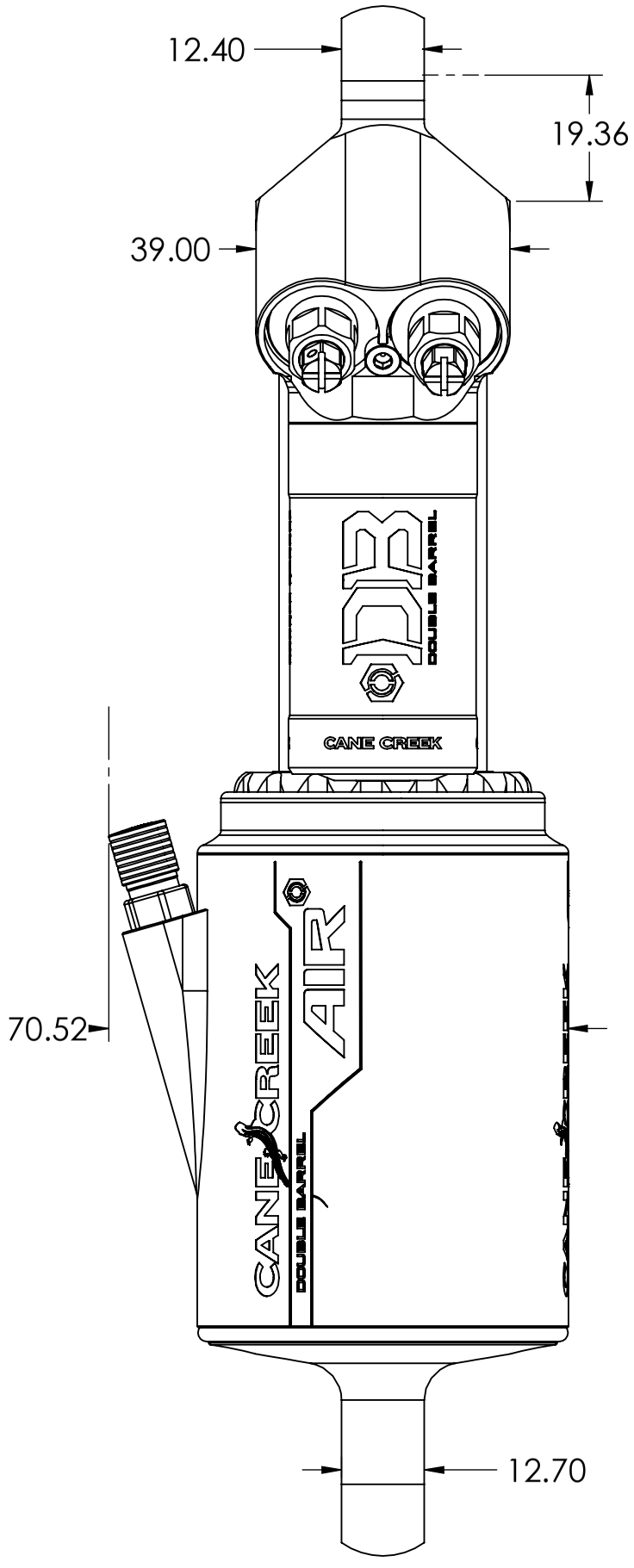

Notes:
1.) Refer to owner's manual for Eye-Eye length and Travel.
2.) Air Can rotates 360°. 70.52mm = Max offset.
3.) 64.91mm Max with adjusters turned full counterclockwise.
4.) 57mm ∅ Max = 59mm ∅ Max for DB Coil.
5.) Available travel may not use full tube length. Varies by shock configuration.

Dimensions Tolerances: .X ± .XX ± .XXX ± Angular: ± Concentricity: Third Angle Projection		CANE CREEK TITLE: DB Air Dimensions
Material:	SIZE B	Part No. REV. 01
Weight:		
Finish:	Color:	SCALE: 1:1 SHEET 1 OF 1

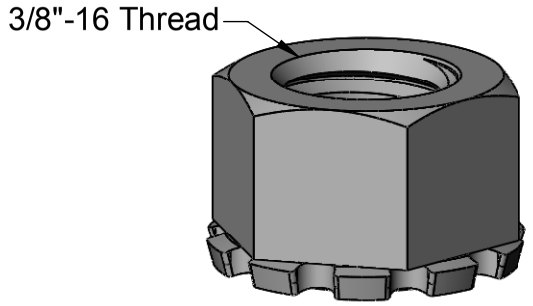

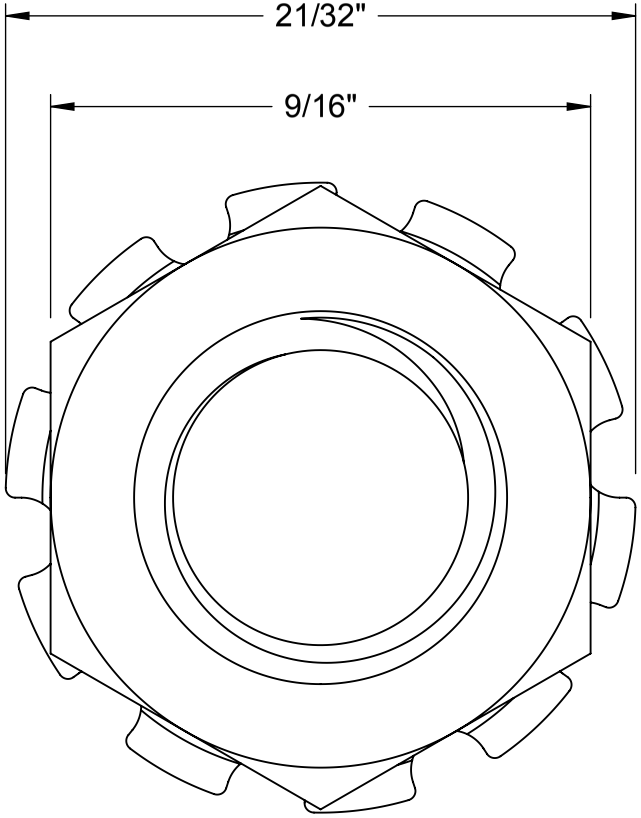

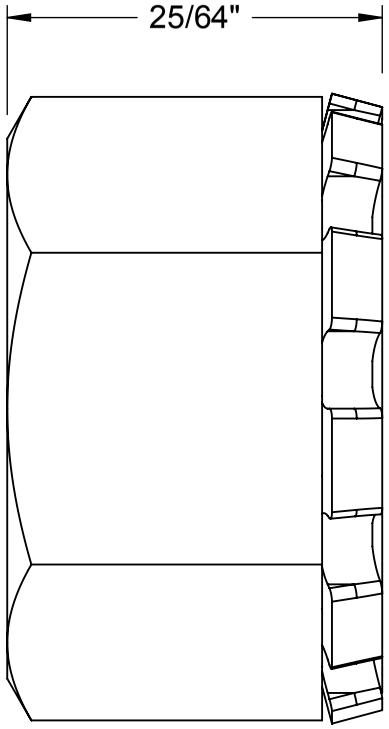

McMASTER-CARR® CAD

http://www.mcmaster.com

PART NUMBER **90675A031**

Hex Nut
with Lock Washer

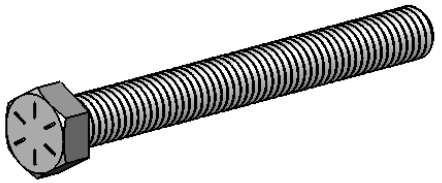

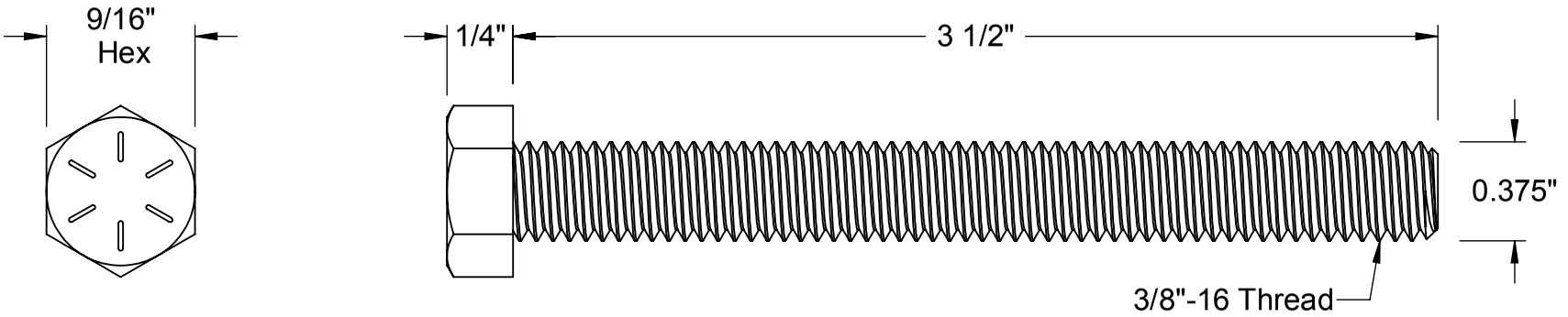

McMASTER-CARR® CAD

http://www.mcmaster.com

PART NUMBER **92620A638**

High-Strength Steel
Cap Screw-Grade 8

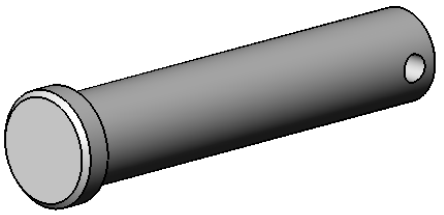

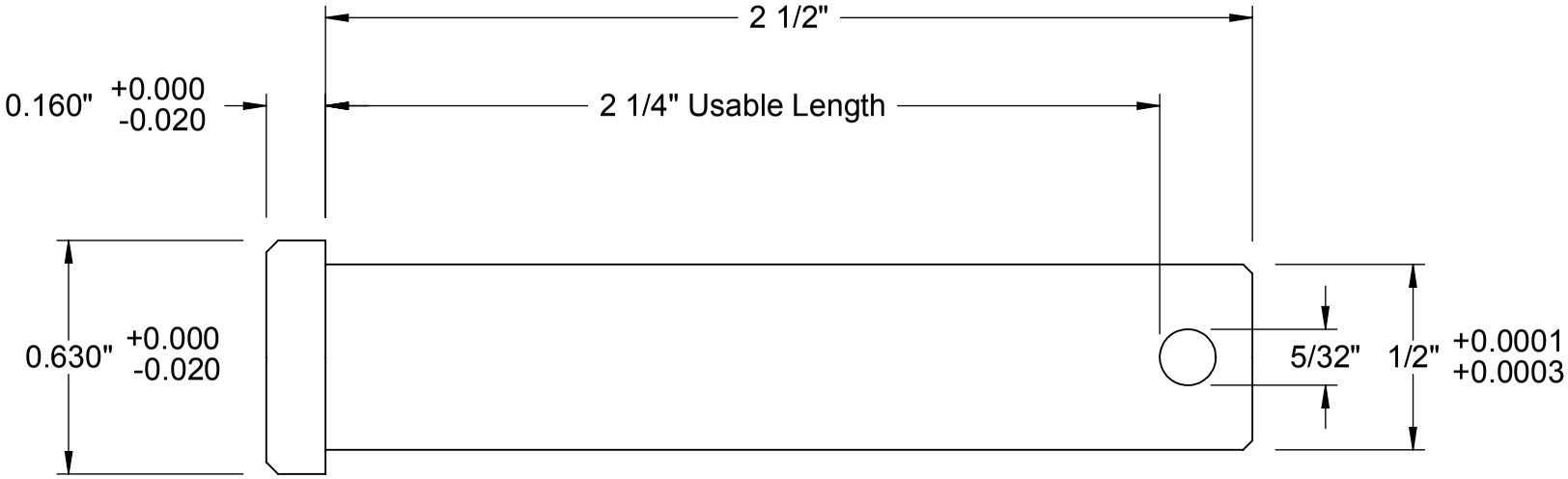

McMASTER-CARR® CAD

http://www.mcmaster.com

PART NUMBER 90378A590

Precision Clevis Pin

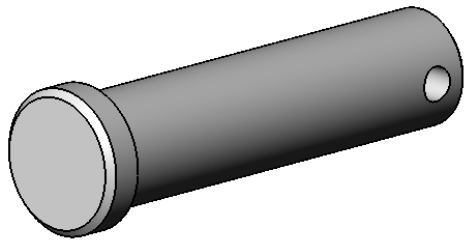

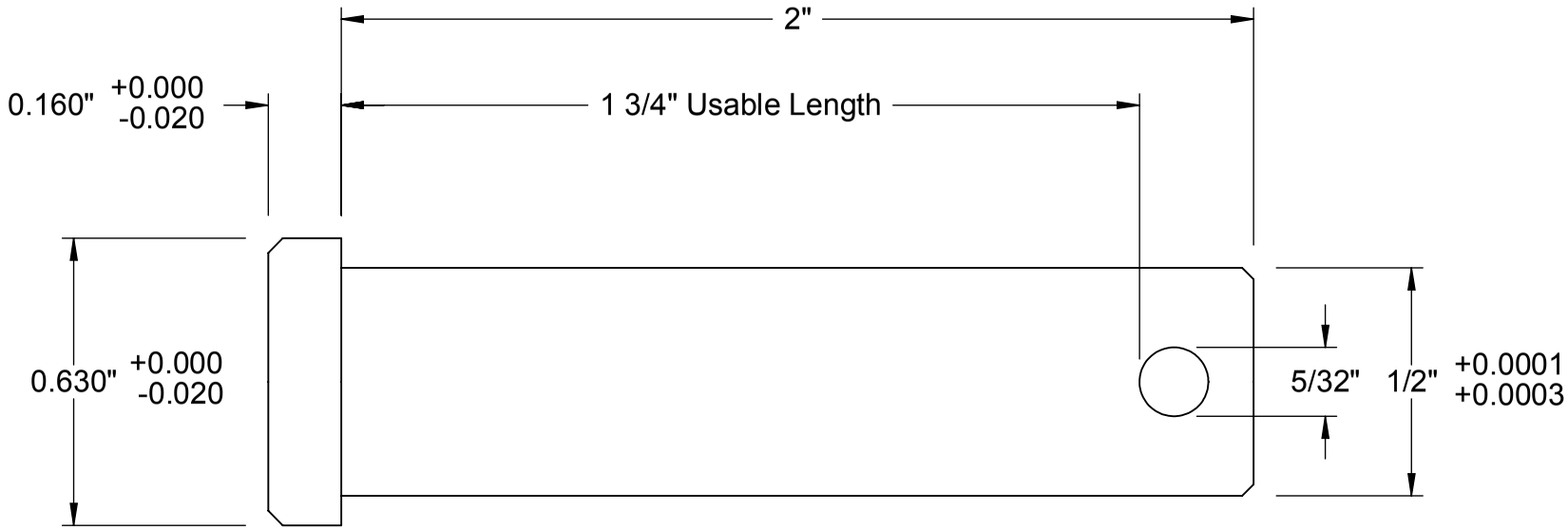

McMASTER-CARR® CAD

http://www.mcmaster.com

PART NUMBER 90378A550

Precision Clevis Pin

Appendix C – Cost Estimate

Table C.1: Cost estimate for suspension system.

Cost Estimate			
	Price Per Unit	Quantity	Total
Item	US Dollars	-	US Dollars
Chromoly Tubing (per foot)	30.42	14	425.88
Bolts (5 Pack)	11.02	7	77.14
Nuts (100 Pack)	10.3	1	10.3
Clevis Pins Short	3.6	8	28.8
Clevis Pins Long	4.13	16	66.08
Cotter Pins (Pack of 50)	14.23	1	14.23
Carbon Tubing (Per 6 Feet)	98.99	2	197.98
6061 Aluminum (per Volume)	27.99	2	55.98
Rod Ends	26.18	16	418.88
Swivel Bearings	26.18	8	209.44
Tube Adapters	5.95	16	95.2
Cane Creek Shock	360	4	1440
Total Price ($)			3039.91

Appendix D – Data Sheets

Rockwest Composites Technical Data

SKU : 45558-HM Rev A		
Ply #	**Orientation**	**Location**
1	0	Inside
2	0	
3	0	
4	45	
5	-45	
6	0	
7	0	
8	90	
9	90	↓
10	0	
11	0	
12	-45	
13	45	
14	0	
15	0	
16	0	
17	0/90	Outside

TUBE - PLAIN WEAVE - HIGH MODULUS - 0.625 X 0.760 X 72 INCH

Round Tubing	ID - Inner Diameter Range (inches)			OD - Outer Diameter Range (inches)			LG - Length (inches)[1]	
	0.250 - 1.875	2.000 - 4.250	4.375 - 6.500	0.375 - 2.000	2.125 - 4.250	4.375 - 6.500	Under 48.00[2]	Over 48.00
Fabric	+/- 0.006	+/- 0.010	+/- 0.013	+/- 0.012	+/- 0.020	+/- 0.025	+/- 0.050	+/- 0.25
Unidirectional								
Texalium								
Torsion								
Hi-Mod								
ZTE								
Sanded Filament Wound	+/- 0.007	+/- 0.010	+/- 0.015	+/- 0.007	+/- 0.010	NA		
Unsanded Filament Wound				+/- 0.030	+/- 0.035	+/- 0.040		
Camera Rails (15mm & 19mm)[3]	+/- 0.006	NA	NA	+/- 0.003	NA	NA		

Shaped Tubing[4]	ID - Inner Flat to Flat Range (inches)	OD - Outer Flat to Flat Range (inches)	LG - Length (inches)[1]	
	0.250 - 2.000	0.750 - 2.250	Under 48.00[2]	Over 48.00
Square	+/- 0.006	+/- 0.020	+/- 0.050	+/- 0.25
Rectangular	+/- 0.006	+/- 0.020	+/- 0.050	+/- 0.25
Hexagonal	+/- 0.008	+/- 0.020	+/- 0.050	+/- 0.25

Notes

1. Current saw capacity allows us to cut up to 4.0" diameter tubes consistently, beyond 4.0" we do not provide a tolerance callout
2. Tighter tolerances (+/- 0.010") available under 48" for additional charge
3. Base size for the 15mm rails is 0.589" OR 14.96mm, Base size for the 19mm rails is 0.746" OR 18.96mm
4. Radius of corners not called out - Typically radius is mentioned if you hover over the part # on the website

Appendix E – Analysis

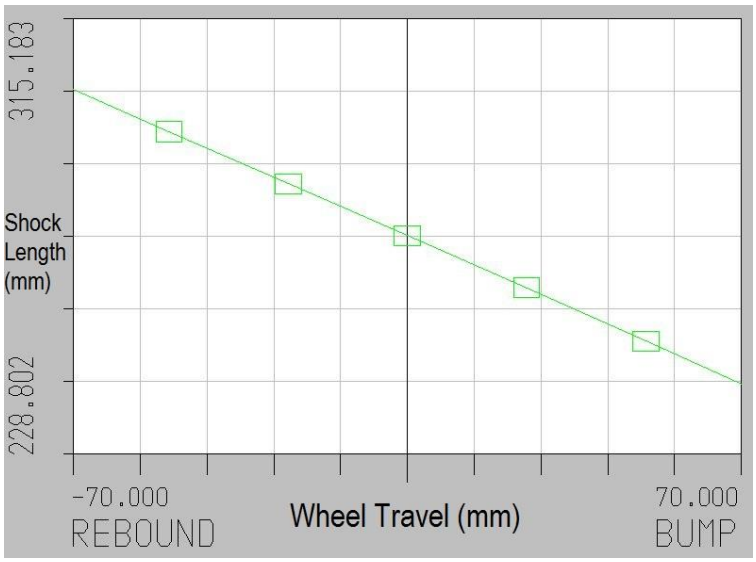

Figure E.1: Shock Length vs Wheel Travel

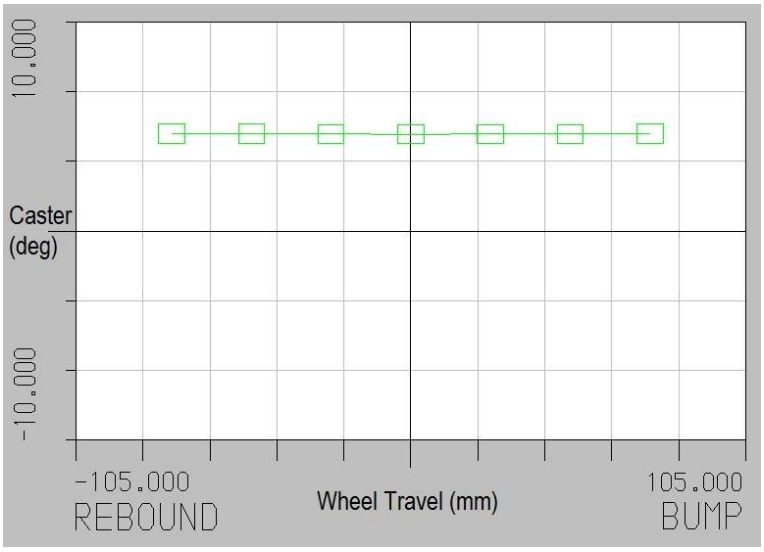

Figure E.2: Caster Angle vs Wheel Travel

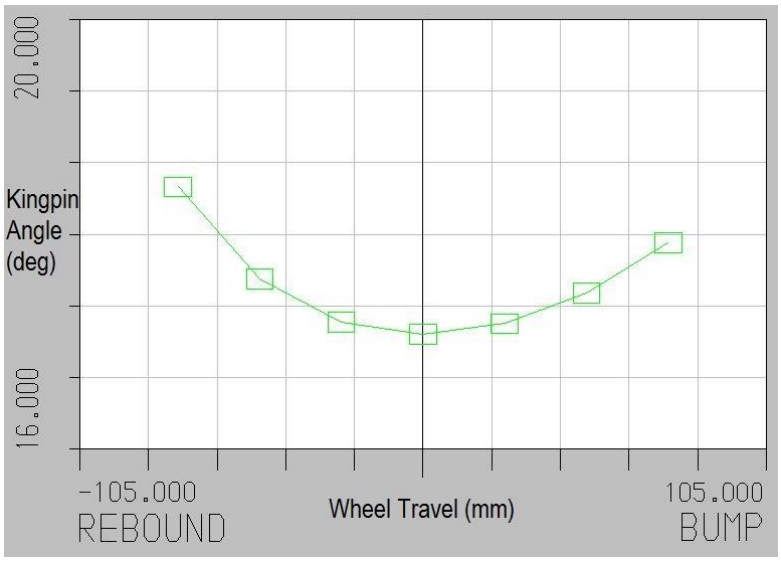

Figure E.3: Kingpin Angle vs Wheel Travel

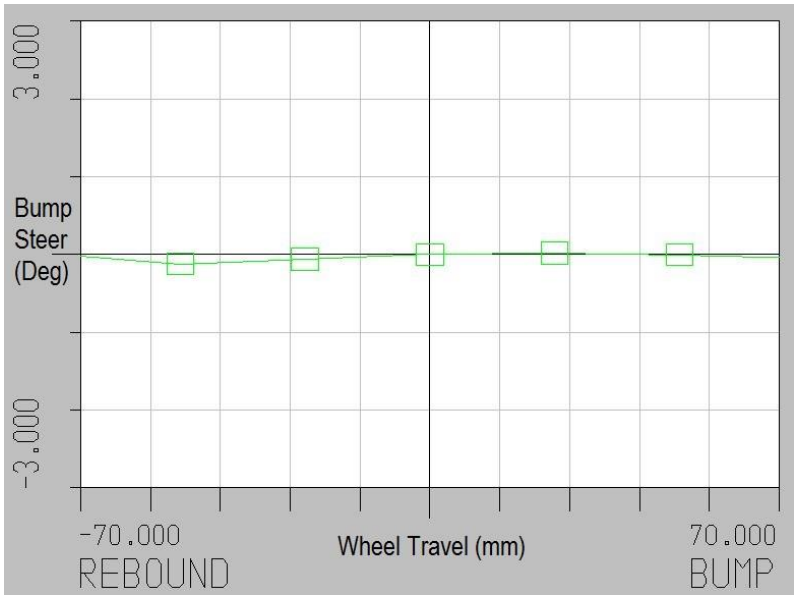

Figure E.4: Bump Steer vs Wheel Travel

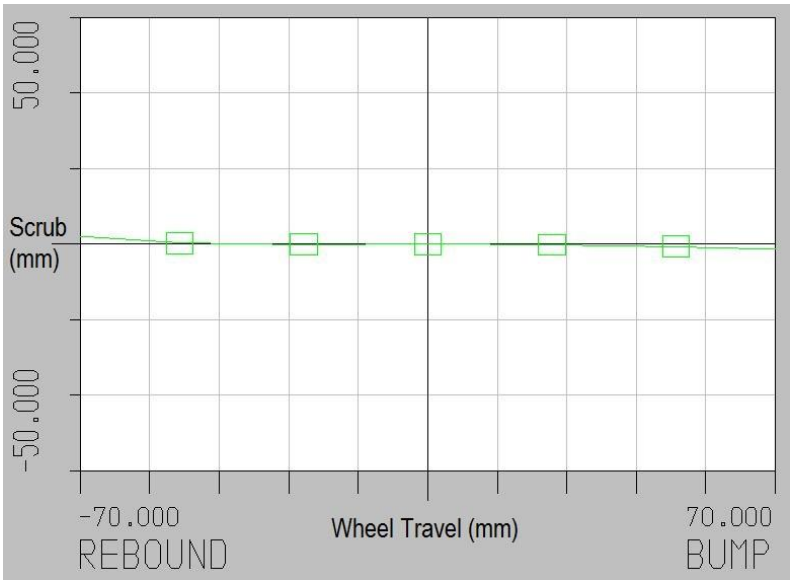

Figure E.5: Scrub vs Wheel Travel

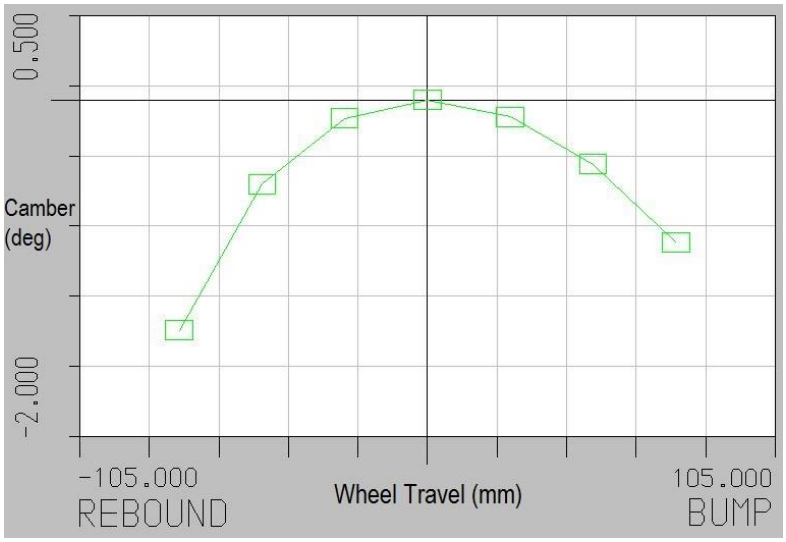

Figure E.6: Camber Angle vs Wheel Travel

UPRIGHT ANALYSIS (1)

→ WORST CASE SCENARIO: SLIDING SIDEWAYS

MATERIAL: 6061-T6 511 ALUMINUM $S_{YIELD} = 40 ksi$

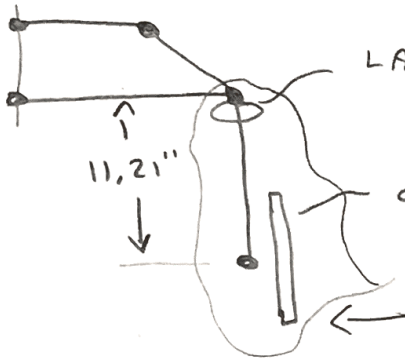

- ASSUME: $N_S = 1$, $W = 500$ lb, WHEEL RIGIDLY ATTACHED TO UPRIGHT

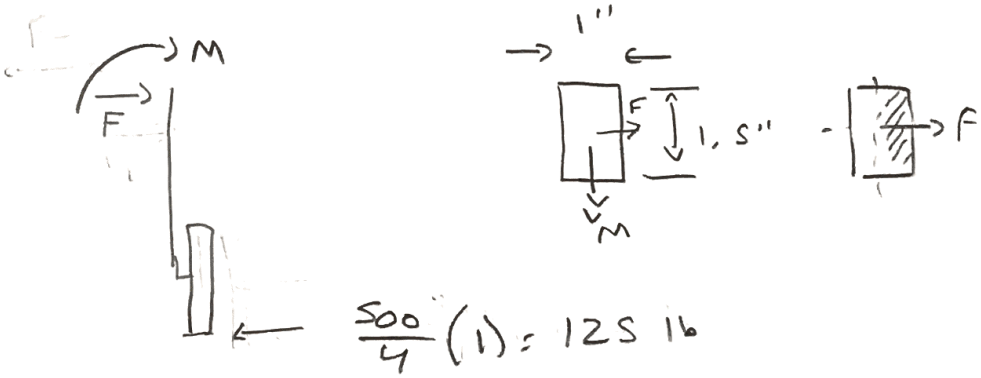

$F = 125$ lb

$M = (125\text{ lb})\left(\frac{20\text{ in}}{2} + 11.21"\right)$

$M = 2651.25$ in-lb

$\sigma_{BND} = \frac{MC}{I} = \frac{(2651.25)(1/2)}{1/12\,(1)(1.5)^3}$

$\sigma_{BND} = 4713.33$ psi

$\tau = \frac{F Q^{A\bar{y}}}{I t} = \frac{(125)(.5)(1.5)(.25)}{1/12\,(1)(1.5)^3(1)}$

$\tau = 83.3$ psi

UPRIGHT ANALYSIS (2)

VON MISES EQUIVALENT

$$\sigma' = \sqrt{\sigma^2 + 3\tau_{xy}^2}$$

$$\sigma' = \sqrt{4713.33^2 + (83.3^2)(3)}$$

$$\sigma' = 4716$$

$$SF = \frac{40{,}000 \text{ psi}}{4716} = \boxed{8.48}$$ AGAINST YIELD

CARBON FIBER ANALYSIS (1)

- WORST CASE SCENARIO: SLIDING SIDEWAYS
- MATERIAL CARBON FIBER

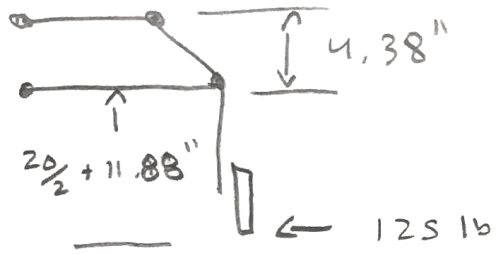

FBD

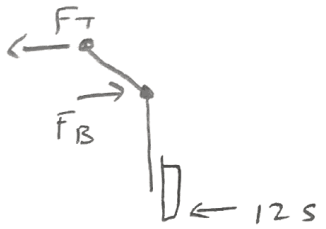

$$\Sigma M_{F_T} = 0 = F_B(4.38) - 125\left(4.38 + \frac{20}{2} + 11.88\right)$$

$$F_B = 750 \text{ lb}$$

$$F_T = 625 \text{ lb}$$

TOP

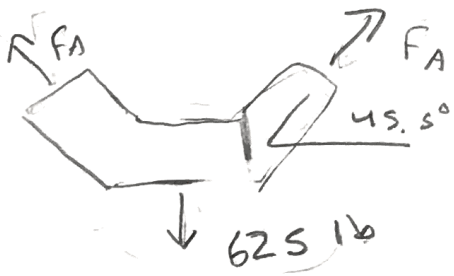

$$\Sigma F = 0 \quad 2F_A \sin 45.5 = 625$$

$$F_A = 438.5 \text{ lb}$$

TENSION

CARBON ANALYSIS (2)

F

BOTTOM

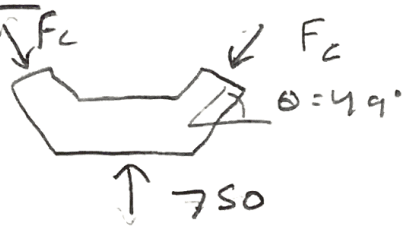

$$2 F_c \sin(49°) = 750$$

$$F_c = 496.88$$

→ DESIGN CARBON AROUND BOTTOM BECAUSE IT SEES HIGHER LOADS AND CARBON IS WORSE IN COMPRESSION

LINE LOAD ANALYSIS

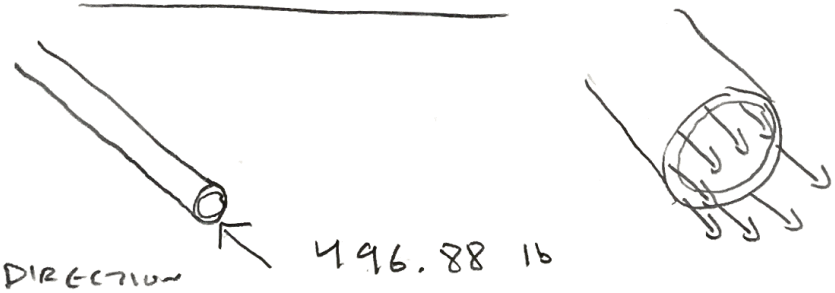

FOR 0 DIRECTION

$$N_{X_{ALL}} = E_{FIBER} \times \varepsilon_x^u \times .8 \times t_{PLY}$$

ALLOWABLE LINE LOAD PER PLY

E_{FIBER} = FIBER MODULUS

ε_x^u = ULTIMATE STRAIN

.8 = PSUEDOMIN (SAFETY FACTOR

t_{PLY} = PLY THICKNESS

$$N_{X_{ALL}} = (15 \times 10^6)(.01)(.8)(.005)$$

$$N_{X_{ALL}} = 600 \text{ lb/in}$$

$$N_{X_{ACTUAL}} = \frac{496.88}{\pi(.625)} = 253.06$$

$$\# \text{ PLYS} = \frac{253.06}{600} = .422 \rightarrow 1 \text{ PLY}$$

CARBON ANALYSIS (3)

WE PURCHASED TUBES WITH 10 PLIES IN 0 DIRECTION

$$FOS = \frac{10}{1} = \boxed{10}$$

EPOXY ANALYSIS (1)

WORST CASE SCENARIO : SLIDING SIDEWAYS

$\sigma_{YIELD\ EPOXY\ (TESTED)} > 2000\ psi$

$F = 496.88\ lb$

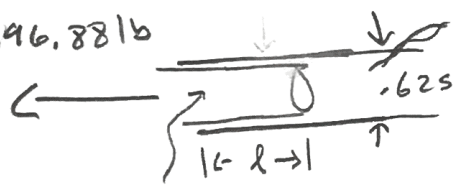

$l = 1.25"$ (BOND LENGTH

$\sigma_{MAX} = \frac{F}{SA} \qquad \frac{F}{\pi D l} = \frac{496.88\ lb}{\pi(.625")(1.25")} = 202\ psi$

SURFACE AREA

$\sigma_{MAX} =$

$FOS = \frac{2000}{202} = \boxed{9.9}$

ROD END ANALYSIS (1)

STEEL $\sigma_{ULT} = 85$ KSI

WCS → 3G BUMP LOAD

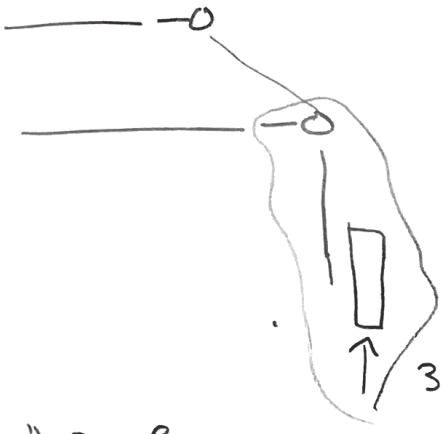

ASSUME: ALL LOADING GOES INTO ONE ROD END (CONSERVATIVE APPROACH)

3G BUMP LOAD $= \frac{3(500)}{4} = 375$ lb

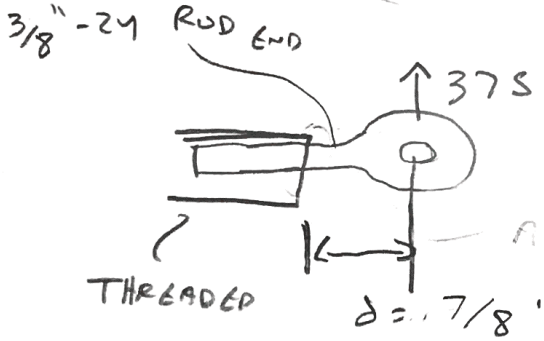

$M = 375\left(\frac{7}{8}\right) = 328.125$ in-lb

$c = \left(\frac{3}{8}\right)\left(\frac{1}{2}\right) = .1875"$

$I = \pi/4\left(\frac{3}{8} \times .5\right)^4 = 9.707 \times 10^{-4}$

$\sigma_{MAX} = \frac{Mc}{I} = 63$ KSI

$\sigma_{ULTIMATE} = 85$ KSI

$FOS = \frac{85}{63} = \boxed{1.35}$

SHOCK CONNECTION

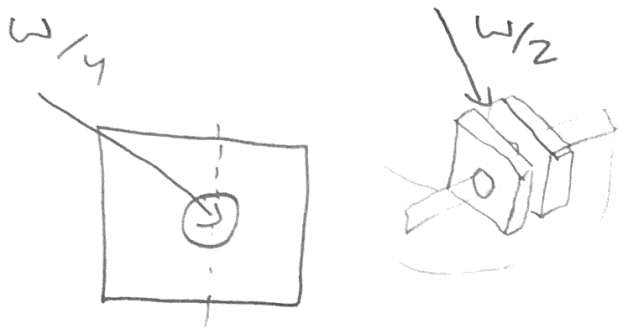

EACH CARRIES $\frac{(W/2)}{2} = \frac{W}{4}$

$V = W/4 \sin\theta_{SHOCK}$

$P = W/4 \cos\theta_{SHOCK}$

$$\tau = \frac{VQ}{It}$$

$$\sigma_{AX} = \frac{P}{A_P}$$

$$\sigma_{BEARING} = \frac{(W/4)}{\left(\frac{\pi}{2} \cdot D \cdot t\right)}$$

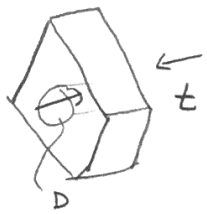

VON MISES EQUIVALENT

CORNER CONNECTION

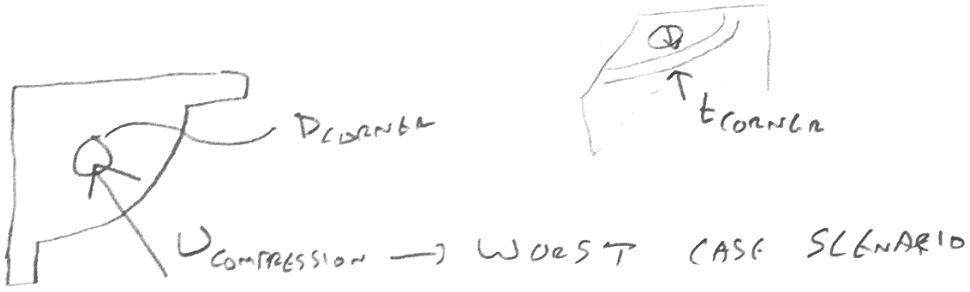

$$\sigma_{BEARING} = \frac{U_{COMPRESSION}}{-\left(\pi/2\right)\left(D_{CORNER}\right)\left(t_{CORNER}\right)}$$

Bolt Analysis

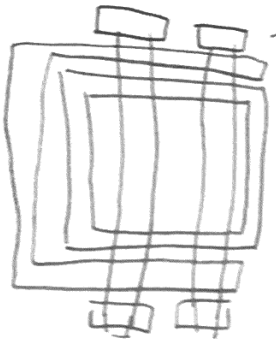

$U_{compression} = 1909$ lb

$U_{tension} = 1559$ lb

Upright

$U_{TS\ Bolts} = 150{,}000$ psi

$$\sigma = \frac{F}{8td} = \frac{1909}{8(.25)(.375)} = 2545 \text{ psi} << 150000$$

$$\tau = \frac{F}{8\pi d^2/4} = \frac{1909}{8\pi\left(\frac{.375^2}{4}\right)} = 2160 \text{ psi} << 150000$$

Shock mount

WCS: 3g Bump Load

$\frac{700 \text{ lb}}{32.2} = 21.7$ slugs

$3g_{Bump} = (21.7)(3)(32.2)$

$F = 2096$ lb

$$\sigma = \frac{F}{3td} = \frac{2096 \text{ lb}}{3(.25)(.375)} = 7452 \text{ psi} << 150000$$

$$\tau = \frac{F}{3\pi d^2/4} = \frac{2096 \text{ lb}}{3\pi\left(\frac{.375^2}{4}\right)} = 6325.8 \text{ psi} << 150000$$

CONTROL ARM

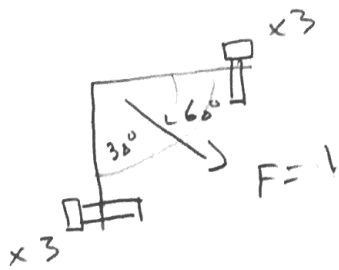

F = 1909 lb

954.5

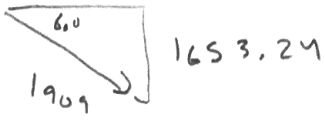

$$\sigma = \frac{1653.24\ lb}{3\,(.25)(.375)}$$

$\sigma = 5880\ psi << 150000$

$$\tau = \frac{1653.24\ lb}{3\pi\left(\frac{.375^2}{4}\right)} = 4992\ psi << 150000$$

ALL BOLTS ARE WELL BELOW YIELD STRENGTH

Stress Analysis of the Chromoly 4130 Upright

Case 1: Sliding Sideways

Input Variables

$D_{wheel} = 22$ [in] *diameter of the wheel*

$w_{upright} = 9$ [in] *total width of the upright*

$w_{tubetotube} = 7$ [in] *upright width from the middle of each tube*

$W_{car} = 600 \cdot 0.8$ [lbf] *Weight of the car and person multiplied by a kinetic coefficient of friction of .8*

$Height_{Upright} = 19$ [in] *Overall Height of the tallest Upright*

$\theta_{insert} = 60$ [deg] *Angle of the Carbon Fiber rods*

$w_{wheel} = 3$ [in] *wheel width*

Mechanical Properties of 6061-T6 Aluminum and 4130 Chromoly

$\sigma_{yield,chromoly} = 75000$ [psi]

$\sigma_{ult,chromoly} = 94000$ [psi]

$\rho_{chromoly} = 0.284$ [lbf/in^3]

$\sigma_{6061,yield} = 40000$ [psi]

Square Cross Section for Chromoly Tubing

$t_{chromoly} = 0.125$ [in]

$b_{chromoly,wide} = 2.5$ [in]

$h_{chromoly,small} = 1.5$ [in]

$h_{welded,joint} = 3.5$ [in] *This is height of the welded support joint in the middle of the upright*

$$I_{1,chrom} = \frac{1}{12} \cdot b_{chromoly,wide} \cdot \left[\frac{h_{chromoly,small}}{2}\right]^3$$ *Moment of Inertia for the outer Rectangle*

$$I_{2,chrom} = \frac{1}{12} \cdot \left[b_{chromoly,wide} - 2 \cdot t_{chromoly}\right] \cdot \left[\frac{h_{chromoly,small}}{2} - t_{chromoly}\right]^3$$ *Moment of Inertia for the inner Rectangle*

$I_{chromoly,end} = I_{1,chrom} - I_{2,chrom}$ *actual moment of inertia for the rectangular tube*

$M_{square,1} = Axle_{coupledforce} \cdot w_{tubetotube}$ *Moment caused by the axle force*

$$M_{square,2} = \frac{W_{car}}{2} \cdot h_{welded,joint}$$ *moment countered by the middle beam*

$M_{square,total} = M_{square,1} - M_{square,2}$ *equivalent moment at the top of the square tubing*

$$\sigma_{new,chrom} = \frac{M_{square,total} \cdot \frac{h_{chromoly,small}}{2}}{I_{chromoly,end}}$$

$$A_{square,1} = \frac{b_{chromoly,wide} \cdot h_{chromoly,small}}{2}$$

$$A_{square,2} = [b_{chromoly,wide} - 2 \cdot t_{chromoly}] \cdot [h_{chromoly,small} - t_{chromoly}]$$

$$\bar{y}_{square,1} = \frac{h_{chromoly,small}}{4}$$ *centroid calculation*

$$\bar{y}_{square,2} = \frac{\frac{h_{chromoly,small}}{2} - t_{chromoly}}{2}$$

$$Q_{square} = A_{square,1} \cdot \bar{y}_{square,1} - A_{square,2} \cdot \bar{y}_{square,2}$$

$$\tau_{new,chrom} = Axle_{coupledforce} \cdot \frac{Q_{square}}{I_{chromoly,end} \cdot 2 \cdot t_{chromoly}}$$

$$\sigma_{vonmises,squareTubing} = \sqrt{\sigma_{new,chrom}^2 + 3 \cdot \tau_{new,chrom}^2}$$ *equivalent von mises stress at the top of the square tubing*

$$FOS_{squareTubing} = \frac{\sigma_{yield,chromoly}}{\sigma_{vonmises,squareTubing}}$$

Chromoly Square Tube Estimated Weight Calculation

$$A_{outer} = b_{chromoly,wide} \cdot h_{chromoly,small}$$

$$A_{inner} = [h_{chromoly,small} - t_{chromoly}] \cdot [b_{chromoly,wide} - 2 \cdot t_{chromoly}]$$

$$Volume_{SquareTubing} = [A_{outer} - A_{inner}] \cdot [w_{upright} - 2 \cdot h_{chromoly,small} + Height_{Upright} \cdot 2]$$

$$Weight_{upright} = \rho_{chromoly} \cdot Volume_{SquareTubing}$$

$$Weight_{Upright,total} = 4 \cdot Weight_{upright}$$

Stress Analysis of the 6061 t6 Aluminum Axle

Axle Moment

$D_{axle} = 0.75$ [in] *Axle will be this big*

$$I_{axle} = \frac{\pi}{4} \cdot \left[\frac{D_{axle}}{2}\right]^4$$

$$M_{axle} = \frac{W_{car}}{2} \cdot \frac{D_{wheel}}{2}$$

$$Slope_{Moment} = \frac{M_{axle}}{\frac{w_{tubetotube}}{2}}$$

$$Axle_{coupledforce} = \frac{M_{axle}}{w_{tubetotube}}$$

$$M_{axle,big} = Slope_{Moment} \cdot \left[\frac{w_{upright}}{2} - h_{chromoly,small} - \frac{w_{wheel}}{2}\right]$$ *Using Beam theory to calculate the equivalent moment at the edge of the wheel*

$$\sigma_{axle,bend} = \frac{M_{axle,big} \cdot \frac{D_{axle}}{2}}{I_{axle}}$$

$$FOS_{axle} = \frac{\sigma_{6061,yield}}{\sigma_{axle,bend}}$$

Reactive Forces at the welded portion of the upright

$$M_{weld} = Axle_{coupledforce} \cdot w_{tubetotube}$$

$$V_{weld} = Axle_{coupledforce}$$

Upright Notch Stress Calculation

Stress acting at the notch for the axle in the upright

$$A_{bearing} = 2 \cdot \frac{\pi}{2} \cdot D_{axle} \cdot t_{chromoly}$$ *Bearing Stress acting at the notch*

$$\sigma_{chromoly,bearing} = \frac{Axle_{coupledforce}}{A_{bearing}}$$

$k_{t,notch} = 5$ [-] *Big Stress Concentration to make sure that the notch doesn't fail*

$$\sigma_{chromoly,notch} = k_{t,notch} \cdot \sigma_{chromoly,bearing}$$

$$FOS_{notch} = \frac{\sigma_{yield,chromoly}}{\sigma_{chromoly,notch}}$$

Weldment Stress Calculation

Shigleys Method of Weld Stress Calculation

$h_{weld} = 0.125$ *h is the weld throat thickness*

$$A_{throat} = 1.414 \cdot h_{weld} \cdot b_{chromoly,wide}$$

$$I_{unit} = \frac{b_{chromoly,wide} \cdot h_{chromoly,small}^{2}}{2}$$ *Unit 2nd Moment of Area for a fillet weld*

$$I_{actual} = 0.707 \cdot h_{weld} \cdot I_{unit}$$ *2nd Moment of Area of the fillet weld*

$$\tau_{primary,weld} = \frac{V_{weld}}{A_{throat}}$$

$$\tau_{secondary,weld} = \frac{M_{weld} \cdot \frac{h_{chromoly,small}}{2}}{I_{actual}}$$

$$\tau_{weld,equivalent} = \sqrt{\tau_{primary,weld}^{2} + \tau_{secondary,weld}^{2}}$$

$\sigma_{yield,weld}$ = 71500 [psi] *properties for ER705-2 Filler Metal for Tig Welding*

$$FOS_{weld,yield} = \frac{\sigma_{yield,weld}}{\tau_{weld,equivalent}}$$ *design against yield*

Stress Analysis of The Carbon Fiber Rods

Using Line Load Analysis on Compression Side of Carbon Rods to estimate the number of plys needed along the axis of the tube

D_{carbon} = 0.75 [in] *Inner Diameter of our Carbon Rods*

$l_{between,Aarms}$ = 5.5 [in]

$$U_{lower,connection} = \frac{W_{car}}{2} \cdot \left[\frac{Height_{Upright} + \frac{D_{wheel}}{2}}{l_{between,Aarms}} \right]$$ *Compression*

$$U_{upper,connection} = \left| \frac{W_{car}}{2} - U_{lower,connection} \right|$$ *Tension*

E_{fiber} = $15 \cdot 10^{6}$ *Engineering Modulus of The fiber in our Carbon Rods*

$\varepsilon_{ultimate,compression}$ = 0.01 [in/in] *Max Strain*

pseudomin = 0.8 [-] *Use a pseudomin to add a safety factor*

t_{ply} = 0.006 [in] *thickness of each carbon fiber cloth ply*

$N_{x,allowable} = E_{fiber} \cdot \varepsilon_{ultimate,compression} \cdot pseudomin \cdot t_{ply}$ *Allowable line load for one ply of fiber*

$$N_{compression} = \frac{U_{lower,connection}}{\pi \cdot D_{carbon}}$$ *Line load applied from our loading condition*

$$n_{carbonfiberplys} = \frac{N_{compression} \cdot 5}{N_{x,allowable}}$$ *Use A large factor of safety for Carbon because it is an anisotropic material*

Stress Analysis of 6061 t-6 Aluminum Inserts at shearing point

$L_{horizontal}$ = 2 [in] *Horizontal Length to Carbon Fiber Rod Connection*

$L_{Vertical}$ = 3 [in] *Vertical Length to Carbon Fiber Rod Connection*

b_{insert} = 1.5 [in]

$h_{insert} = 1.25$ [in]

$A_{insert,cross} = b_{insert} \cdot h_{insert}$

$$Q_{insert} = \frac{h_{insert}}{4} \cdot \frac{A_{insert,cross}}{2}$$

$$I_{insert} = \frac{1}{12} \cdot b_{insert} \cdot h_{insert}^{3}$$

$t_{insert} = b_{insert}$

$M_{insert} = \left| U_{lower,connection} \cdot \sin\left[\theta_{insert}\right] \cdot L_{horizontal} - U_{lower,connection} \cdot \cos\left[\theta_{insert}\right] \cdot L_{Vertical} \right|$ *Moment exerted on the the aluminum inserts at the ang e*

$insert_{shear} = U_{lower,connection} \cdot \sin\left[\theta_{insert}\right]$

$insert_{axial} = U_{lower,connection} \cdot \cos\left[\theta_{insert}\right]$

$$\sigma_{insert,axial} = \frac{insert_{axial}}{A_{insert,cross}}$$

$$\sigma_{insert,shear} = insert_{shear} \cdot \frac{Q_{insert}}{I_{insert} \cdot t_{insert}}$$

$$simga_{insert,bend} = \frac{M_{insert} \cdot \frac{b_{insert}}{2}}{I_{insert}}$$

$$\sigma_{insert,vonmises} = \sqrt{\left[simga_{insert,bend} + \sigma_{insert,axial}\right]^2 + 3 \cdot \sigma_{insert,shear}^{2}}$$

$$FOS_{yield,insert} = \frac{\sigma_{6061,yield}}{\sigma_{insert,vonmises}}$$

Stress Analysis of 6061 t6 bottom insert shock Connection

$\theta_{shock} = 30$ [deg] *Shock angle*

$K_t = 2.5$ [-] *Stress concentration factor from Shigleys Design Book*

$D_{shockconnection} = 0.5$ [in]

$w_{shockconnection} = 0.5$ [in] *width of the shock connection*

$h_{shockconnection} = 1$ [in]

$l_{shockconnection} = 1.5$ [in] *length of the shock connection*

$h_{ins} = 1.25$ [in] *height of the insert*

$$A_{shock,1} = \left[h_{ins} + \frac{h_{shockconnection}}{2}\right] \cdot w_{shockconnection}$$

$$A_{shock,2} = \frac{D_{shockconnection}}{2} \cdot w_{shockconnection}$$

$A_{tot,shock} = A_{shock,1} - A_{shock,2}$ *Equivalent Area*

$$\bar{y}_{shock} = \frac{A_{shock,1} \cdot \left[\frac{h_{ins} + \frac{h_{shockconnection}}{2}}{2}\right] - A_{shock,2} \cdot \frac{D_{shockconnection}}{4}}{A_{tot,shock}}$$

$$Q_{shock} = \bar{y}_{shock} \cdot A_{tot,shock}$$

$$I_{shock} = \frac{1}{12} \cdot w_{shockconnection} \cdot \left[\frac{h_{shockconnection} + h_{ins} - D_{shockconnection}}{2}\right]^3$$

$$A_{axial} = \left[\frac{l_{shockconnection} - D_{shockconnection}}{2}\right] \cdot w_{shockconnection}$$

$$Insert_{hole,shear} = \frac{W_{car}}{4} \cdot \sin\left[\theta_{shock}\right]$$

$$Insert_{hole,axial} = \frac{W_{car}}{4} \cdot \cos\left[\theta_{shock}\right]$$

$$\sigma_{bearing,shock} = \frac{\frac{W_{car}}{2}}{2 \cdot \frac{\pi}{2} \cdot D_{shockconnection} \cdot w_{shockconnection}}$$

$$\sigma_{shock,shear} = Insert_{hole,shear} \cdot \frac{Q_{shock}}{I_{shock} \cdot w_{shockconnection}}$$

$$\sigma_{shock,axial} = \frac{Insert_{hole,axial}}{A_{axial}}$$

$$\sigma_{shock,equiv} = K_t \cdot \left[\sqrt{\sigma_{shock,axial}^2 + 3 \cdot \sigma_{shock,shear}^2 + \sigma_{bearing,shock}^2}\right]$$

$$FOS_{shockconnection} = \frac{\sigma_{6061,yield}}{\sigma_{shock,equiv}}$$

Stress Analysis of the Corner Connection Points

$t_{corner} = 0.15$ [in] *thickness of the corner connection*

$D_{corner,hole} = 0.5$ [in] *Hole Diameter*

$$\sigma_{connection,bearing} = \frac{U_{lower,connection}}{\frac{\pi}{2} \cdot D_{corner,hole} \cdot t_{corner}}$$ *Bearing Stress Calculation*

$$FOS_{corner} = \frac{\sigma_{6061,yield}}{\sigma_{connection,bearing}}$$

SOLUTION

Unit Settings: Eng F psia mass deg

$Axle_{coupledforce}$ = 377.1 [lbf]
FOS_{axle} = 1.464 [-]
FOS_{notch} = 11.71 [-]
$FOS_{squareTubing}$ = 2.084 [-]
$FOS_{yield,insert}$ = 19.73 [-]
$Insert_{hole,shear}$ = 60 [lbf]
M_{axle} = 2640 [in-lbf]
M_{insert} = 303.8 [in-lbf]
$M_{square,2}$ = 840 [in-lbf]
M_{weld} = 2640 [in-lbf]
$N_{compression}$ = 555.6 [lbf/in]
$\sigma_{6061,yield}$ = 40000 [psi]
$\sigma_{bearing,shock}$ = 305.6 [psi]
$\sigma_{chromoly,notch}$ = 6403 [psi]
$\sigma_{insert,axial}$ = 349.1 [psi]
$\sigma_{insert,vonmises}$ = 2028 [psi]
$\sigma_{shock,axial}$ = 415.7 [psi]
$\sigma_{shock,shear}$ = 3224 [psi]
$\sigma_{vonmises,squareTubing}$ = 35989 [psi]
$\sigma_{yield,weld}$ = 71500 [psi]
$\tau_{new,chrom}$ = -9445 [psi]
$\tau_{secondary,weld}$ = 7966 [psi]
θ_{insert} = 60 [deg]
$U_{lower,connection}$ = 1309 [lbf]
$Volume_{SquareTubing}$ = 28.88 [in^3]
$Weight_{Upright,total}$ = 32.8 [lbf]

D_{axle} = 0.75 [in]
FOS_{corner} = 3.6 [-]
$FOS_{shockconnection}$ = 2.853 [-]
$FOS_{weld,yield}$ = 8.925 [-]
$insert_{axial}$ = 654.5 [lbf]
$insert_{shear}$ = 1134 [lbf]
$M_{axle,big}$ = 1131 [in-lbf]
$M_{square,1}$ = 2640 [in-lbf]
$M_{square,total}$ = 1800 [in-lbf]
$n_{carbonfiberplys}$ = 3.858 [-]
$N_{x,allowable}$ = 720 [lbf/in]
$\sigma_{axle,bend}$ = 27318 [psi]
$\sigma_{chromoly,bearing}$ = 1281 [psi]
$\sigma_{connection,bearing}$ = 11112 [psi]
$\sigma_{insert,shear}$ = 907 [psi]
$\sigma_{new,chrom}$ = 32056 [psi]
$\sigma_{shock,equiv}$ = 14021 [psi]
$\sigma_{ult,chromoly}$ = 94000 [psi]
$\sigma_{yield,chromoly}$ = 75000 [psi]
$simga_{insert,bend}$ = 933.2 [psi]
$\tau_{primary,weld}$ = 853.5 [psi]
$\tau_{weld,equivalent}$ = 8012 [psi]
t_{corner} = 0.15 [in]
$U_{upper,connection}$ = 1069 [lbf]
V_{weld} = 377.1 [lbf]
W_{car} = 480 [lbf]

No unit problems were detected.

Appendix F – Failure Mode Effects Analysis

									Action Results			
Item / Function	**Potential Failure Mode**	**Potential Effect(s) of Failure**	**Sev**	**Potential Cause(s) / Mechanism(s) of Failure**	**Occur**	**Crit**	**Recommended Action(s)**	**Responsibility & Target Completion Date**	**Actions Taken**	**Sev**	**Occur**	**Crit**
Upright must support car and keep wheel centered inside fairing	Excesive Deflection/Yeild	Tire or suspension rubs on fairing; steering is impared; suspension does not track properly	7	Not enough space in fairing; upright tubing too thin			FEA					
	Fracture	Fairing hits ground, wheel, and/or the upright; car cannot be steered; suspension no longer supports car	9	Tubing is too thin; weak welds			Test welds?					
Aluminium joints must join carbon tubes, upright and shock, allow for full suspension travel, and maintain correct suspension geometry	Excesive Deflection/Yeild	Suspension parts or wheel hit fairing or chassis; steering is impaired; suspension doesn't track properly	7	Joint is not thick enough			FEA					
	Fracture	Fairing hits ground, wheel, and/or the upright; car cannot be steered; suspension no longer supports car	9	Joint is not thick enough								
	Carbon/Aluminium bond failure	Fairing hits ground, wheel, and/or the upright; car cannot be steered; suspension no longer supports car	10	Incorrect bonding technique; epoxy is not strong enough			Pull Testing					
Carbon tubes must maintain correct suspension geometry	Fracture	Fairing hits ground, wheel, and/or the upright; car cannot be steered; suspension no longer supports car	10	Tubes are not thick enough or have incorrect ply orientation								
	Incorrect geometry	Suspension does not track correctly	7	Tubes are the wrong lengths			Prototype to verify geometry					
Brackets must connect suspension and shock to chassis and support weight of car	Fracture	Fairing hits ground, wheel, and/or the upright; car cannot be steered; suspension no longer supports car	9	Bracket is too thin			FEA					
	Bolt Failure	Fairing hits ground, wheel, and/or the upright; car cannot be steered; suspension no longer supports car	9	Bolts are not the correct size or material								

Appendix G - References

[1] "Fastest Solar-powered Vehicle." *Guinness World Records*. N.p., n.d. Web. 02 Feb. 2016. <http://www.guinnessworldrecords.com/world-records/fastest-solar-powered-vehicle>.

[2] Official list of world speed records homologated by the FIA in category A. N.d. Raw data. N.p.

[3] Harris, William. "How Car Suspensions Work." *HowStuffWorks*. HowStuffWorks, 11 May 2005. Web. 06 Jan. 2016. <http://auto.howstuffworks.com/car-suspension.htm>.

[4] "Automobile Ride, Handling, and Suspension Design." *Automobile Ride, Handling, and Suspension Design*. N.p., n.d. Web. 02 Feb. 2016. <http://www.rqriley.com/suspensn.htm>.

[5] Bycroft, Luke. *Sunswift IV Front Suspension Design Report*. Rep. N.p.: n.p., 2009. Print.

[6] Digital image. *How to Correct Bump Steer*. N.p., n.d. Web. <http://www.onallcylinders.com/wp-content/uploads/2014/06/bump-steer-pro-touring1.jpg>.

[7] Digital image. N.p., n.d. Web. 2 Feb. 2016. <http://www.fitzhughmedia.com/MBF/photos/W208-2-02.jpg>.

[8] Toe Angle. Digital image. N.p., n.d. Web. 2 Feb. 2016. <http://www.car-engineer.com/wp-content/uploads/2012/07/ToeAngle.png?46ac1a>.

[9] Rear Suspension Model. Digital image. N.p., n.d. Web. 2 Feb. 2016. <http://helix.gatech.edu/classes/ME4182/2000S1/Webs/SunSpension/Image26.jpg>.

[10] Kojima, Mike. "Bump Steer/Toe Steer." *MotoIQ*. MotoIQ, 02 Sept. 2014. Web. 31 Jan. 2016. <http://www.motoiq.com/MagazineArticles/ID/3608/The-Ultimate-Guide-to-Suspension-and-Handling--Bump-SteerToe-Steer.aspx>.

[11] Carlone, P., G.S. Palazzo, and R. Pasquino. *Pultrusion Manufacturing Process Development*. Rep. Fisciano, Italy: U of Salerno, 2006. Print.

[12] Cobi, Albon C.*Design of a Carbon Fiber Suspension System for FSAE Applications*. Thesis. Massachusetts Institute of Technology, 2012. N.p.: Massachusetts Institute of Technology, 2012. Print.

[13] Digital image. *Pultruded Carbon Fiber Tube*. N.d. Web. 29 Feb.2016. <*www.easycomposites.co.uk*>.

[14] Digital image. *Roll Wrapped Carbon Fiber Tube*. N.d. Web. 29 Feb.2016. <*www.professional-multirotors.com*>.

[15] Digital image. N.p., n.d. Web. 29 Feb.2016. <carbonfibertubeshop.com>.

[16] "Production Processes." *GW Composites*. GW Composites, n.d. Web. 20 Feb. 2016. <http://gwcomposites.com/production-processes/carbon-wrapping/>.

[17] Digital image. *Filament Winding*.N.d. Web.29 Feb. 2016. < http://www.nuplex.com>.

[18] *Rockwest Composites*. N.p., n.d. Web. 29 Feb. 2016. <http://www.rockwestcomposites.com/>.

[19] Digital image. *Male Rod End*.N.d. Web.29 Feb. 2016. < http://www.use-enco.com>.

[20] Digital image. 4 Wheel Parts. N.p., n.d. Web. 3 May 2016.

[21] "Aluminum Adhesion." *Epoxyworks*. N.p., 12 Nov. 2015. Web. 12 Dec. 2016.